

# We are IntechOpen, the world's leading publisher of Open Access books Built by scientists, for scientists

**4,800**

Open access books available

**122,000**

International authors and editors

**135M**

Downloads

Our authors are among the

**154**

Countries delivered to

**TOP 1%**

most cited scientists

**12.2%**

Contributors from top 500 universities



**WEB OF SCIENCE™**

Selection of our books indexed in the Book Citation Index  
in Web of Science™ Core Collection (BKCI)

Interested in publishing with us?  
Contact [book.department@intechopen.com](mailto:book.department@intechopen.com)

Numbers displayed above are based on latest data collected.

For more information visit [www.intechopen.com](http://www.intechopen.com)



# Superstrate Antennas for Wide Bandwidth and High Efficiency for 60 GHz Indoor Communications

Hamsakutty Vettikalladi, Olivier Lafond and Mohamed Himdi  
*Institute of Electronics and Telecommunication of Rennes (IETR)*  
*University of Rennes 1*  
*France*

## 1. Introduction

Modern multimedia applications demand higher data rates and the trend towards wireless is evident, not only in telephony but also in home and office networking and customer electronics. This has been recently proven by the accelerating sales of IEEE 802.11 family WLAN hardware. Current WLANs are, however, capable of delivering only 30-100 Mb/s connection speeds, which is insufficient for future applications like wireless high-quality video conferencing, multiple simultaneous wireless IEEE 1394 (Firewire) connections or wireless LAN bridges across network segments. For these and many other purposes, more capacity – wirelessly – is needed. Service provided by IEEE 802.11 WLANs fulfills casual internet users and office workers actual needs. But, bandwidth demands are still rising. Millimetre-wave technology is one solution to provide up to multi-Gbps wireless connectivity for short distances between electronic devices. The data rate is expected to be 40-100 times faster than today's wireless LAN systems, transmitting an entire DVD's data in roughly 15 seconds. 60 GHz is ideally suited for personal area network (PAN) applications. A 60 GHz link can replace various cables used today in the office or in home by wireless link as shown in Fig.1, including gigabit Ethernet (1000Mbps), USB 2.0 (480Mbps), or IEEE 1394 (~800Mbps). Currently, the data rates of these connections have precluded wireless links, since they require so much bandwidth. While other standards are evolving to address this market (802.11n and UWB), 60 GHz is another viable candidate. In such a context, 60 GHz millimeter wave (MMW) systems constitute a very attractive solution due to the fact that there is a several GHz unlicensed frequencies range available around 60 GHz, almost worldwide. In Europe, the frequency ranges 62 - 63 GHz and 65 - 66 GHz are reserved for wideband mobile networks (MBS, Mobile Broadband System), whereas 59 - 62 GHz range is reserved for wideband wireless local area networks (WLAN). In the USA and South Korea, the frequency range 57 - 64 GHz is generally an unlicensed range. In Japan, 59 - 66 GHz is reserved for wireless communications (Nesic et al., 2001). This massive spectral space enables densely situated, non-interfering wireless networks to be used in the most bandwidth-starving applications of the future, in all kinds of short-range (< 1 km) wireless communication. Also in this band, the oxygen absorption reaches its maximum value (10-15 dB/km), which gives an additional benefits of reduced co-channel interference. Hence, it is a

promising candidate for fulfilling the future needs for very high bandwidth wireless connections. It enables up to gigabit-scale connection speeds to be used in indoor WLAN networks or fixed wireless connections in metropolitan areas.



Fig. 1. Short range communication.

These new systems will need compact and high efficient millimeter wave front-ends including antennas. For antennas, printed solutions are often demanding for the researchers because of its low profile, lightweight and ease of integration with active components (Zhang et al., 2006). High gain and high efficient antennas are needed for 60 GHz communication due to high path losses at this range of frequencies. Conventional antenna arrays are used for high gain applications. But in these cases for achieving high gain, a large number of elements are needed, which not only increases the size of the antenna but also decreases its efficiency (Lafond et al., 2001), (Kärnfelt et al., 2006) & (Soon-soo oh et al., 2004). It has been reported that for high gain, a superstrate layer can be added at a particular height of  $0.5 \lambda_0$  above the ground plane (Choi et al., 2003), (Menudier et al., 2007) & (Meriah et al., 2008).

## 2. Superstrate antenna technology

In this chapter the authors are explaining how to develop a wideband, high gain and high efficient antenna sufficient for 60 GHz communications using superstrate technology. Also explains the importance of different sources on antenna performance in terms of bandwidth, gain and efficiency.

### 2.1 Microstrip fed parasitic patch antenna with superstrate

Here the antenna configuration consists of a microstrip feed, patch and a parasitic patch, as the source, which are loaded by a superstrate. Fig. 2 shows the 3D view (a) and side view (b)

of the microstrip fed stacked patch antenna with superstrate. It consists of a lower patch with an optimised dimension of 1.63 mm  $\times$  1.63 mm on a substrate RT Duroid 5880 ( $\epsilon_r = 2.2$ ,  $t_1 = 0.127$  mm). The upper patch with an optimised dimension of 1.63 mm  $\times$  1.63 mm is printed on the lower side of a parasitic substrate RT Duroid 5880 ( $\epsilon_r = 2.2$ ,  $t_2 = 0.254$  mm).

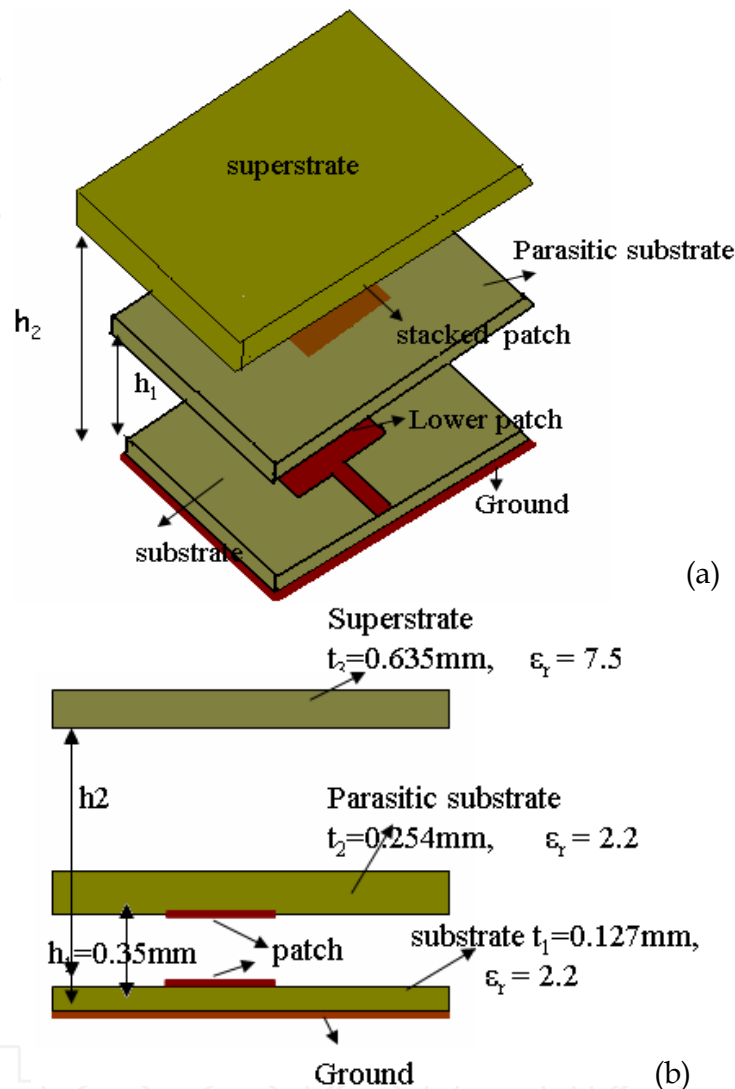
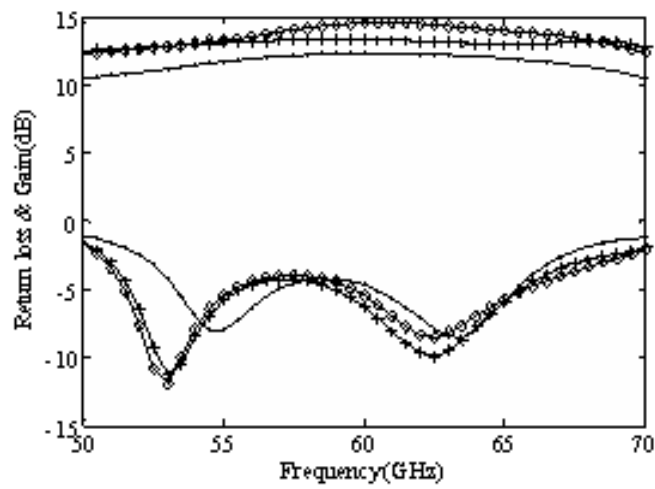
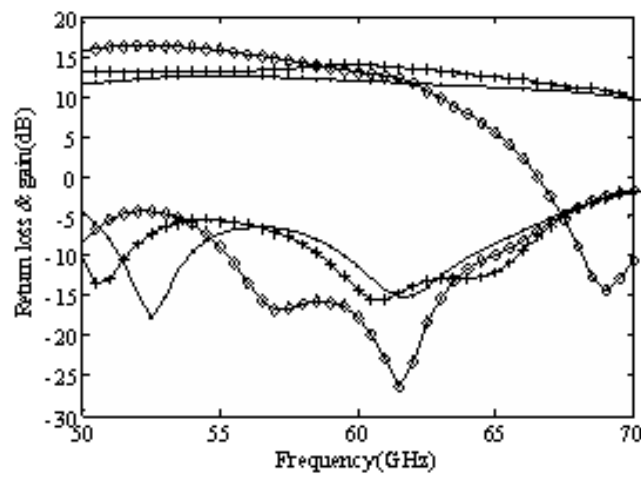


Fig. 2. Cutting plane of stacked patch antenna with superstrate.

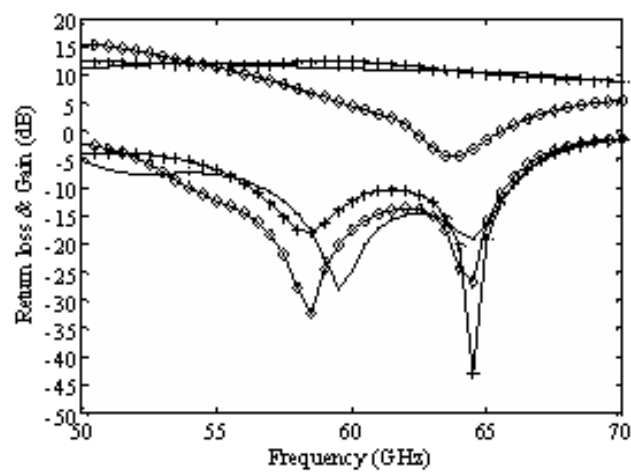
The distance between the lower patch and the upper patch is optimized, by simulation using CST Microwave Studio®, as  $h_1 = 0.35$  mm for a resonance at 60 GHz for a larger bandwidth and gain. This antenna is then loaded with superstrate. The material used for the superstrate is Roger substrate RT6006 ( $\epsilon_r = 7.5$  at 60 GHz,  $t = 0.635$  mm). The dimension of the superstrate and the height from the ground plane are optimized as explained below. The variation of gain and VSWR bandwidth with the variation of superstrate dimension ( $0.73\lambda_0$ ,  $1.1\lambda_0$ ,  $2\lambda_0$ ) for different heights ( $0.5\lambda_0$ ,  $0.6\lambda_0$ ,  $0.7\lambda_0$ ) is shown in Figs. 3 (a-c). It is noted that the maximum gain with good bandwidth is achieved for a superstrate dimension of  $1.1\lambda_0$  with a height =  $0.6\lambda_0$ , and is equal to 13.6 dB with almost flat over a frequency range of 59 GHz to 64 GHz (Vettikalladi et al., 2009). In all other cases either the gain is less than the above value or the VSWR bandwidth is poor. Also noted that when the superstrate dimension is higher than  $1.1\lambda_0$ , the gain goes down when the height  $h_2$  varies from  $0.5\lambda_0$  to  $0.7\lambda_0$ .



(a)



(b)



(c)

Fig. 3. variation of  $s_{11}$  and gain with superstrate dimension and height from ground plane.  
 a)  $h_2=0.5 \lambda_0$  b)  $h_2=0.6 \lambda_0$  c)  $h_2=0.7 \lambda_0$  for size  $=.73 \lambda_0$  —●— size  $=1.1 \lambda_0$  —+—  
 size  $=2 \lambda_0$  —◇— .

From the literature (Gupta et al., 2005), the theoretical height between the superstrate and ground plane is  $0.5\lambda_0$ , but in this work it is found to be  $0.6\lambda_0$  for maximum gain, it may be due to the stacked patch. Fig. 4 shows the return loss, simulated directivity with theoretical values, and simulated and measured gain of the prototype with superstrate. It is found that there is a gain reduction in the measurement, which is due to the variation of exact heights from the theoretical values as shown in Table I.

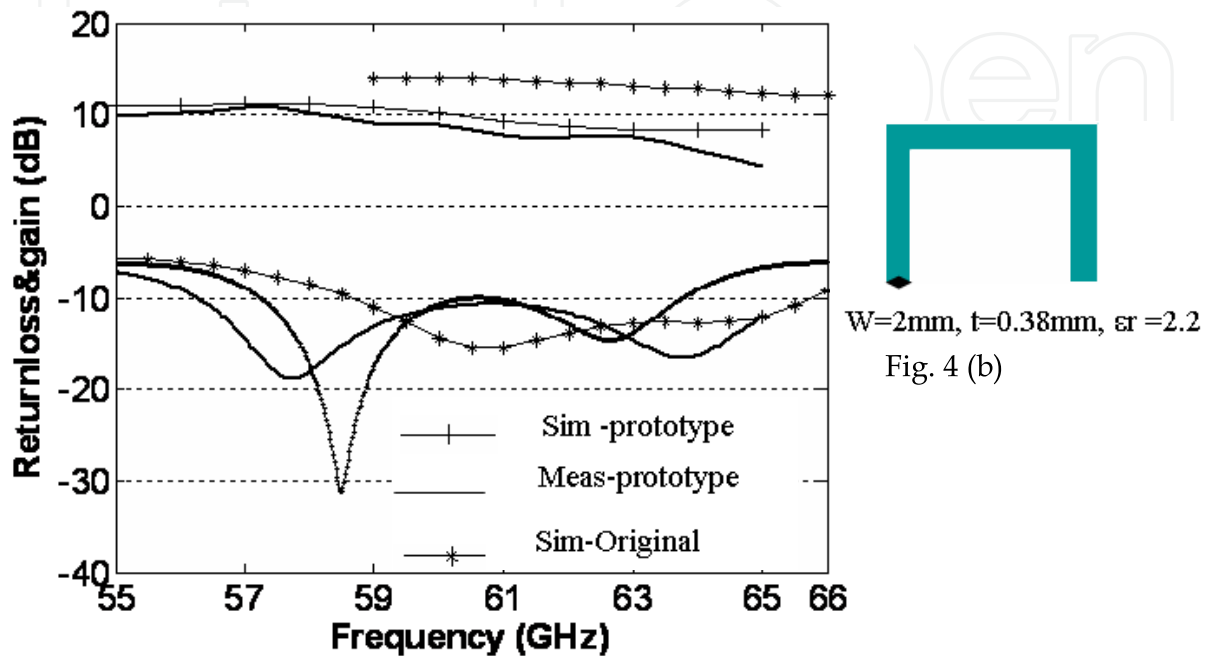


Fig. 4. (a) Comparison of return loss and gain with superstrate.

	Original (mm)	variation while implementation (mm)
Lower Patch	1.6x1.63	1.62x1.65
Upper Patch	1.63x1.63	1.65x1.65
h1	0.35	0.38
h2	3	3.48

Table I. Variation of prototype parameters from exact values.

It is very difficult to maintain the exact thickness  $h_1$ , hence we inserted a substrate cut in the form of a rectangular U shape (Fig. 4(b)), with width 2mm, thickness 0.38mm and permittivity 2.2. Also the thickness  $h_2$  is varied to 3.48mm instead of 3mm ( $0.6\lambda_0$ ) and hence is the reason for the reduction of gain to nearly 10 dB. The E and H planes radiation patterns at 57 GHz and 58 GHz are shown in Figs. 5(a-b). The radiation patterns are found to be broad. There is a cross polar level of less than -20 dB on both the planes. The measured half-power beam widths are found to be  $37^\circ$  for E and H planes at 57 GHz, and  $38^\circ$  and  $41^\circ$  for E and H planes respectively at 58 GHz.

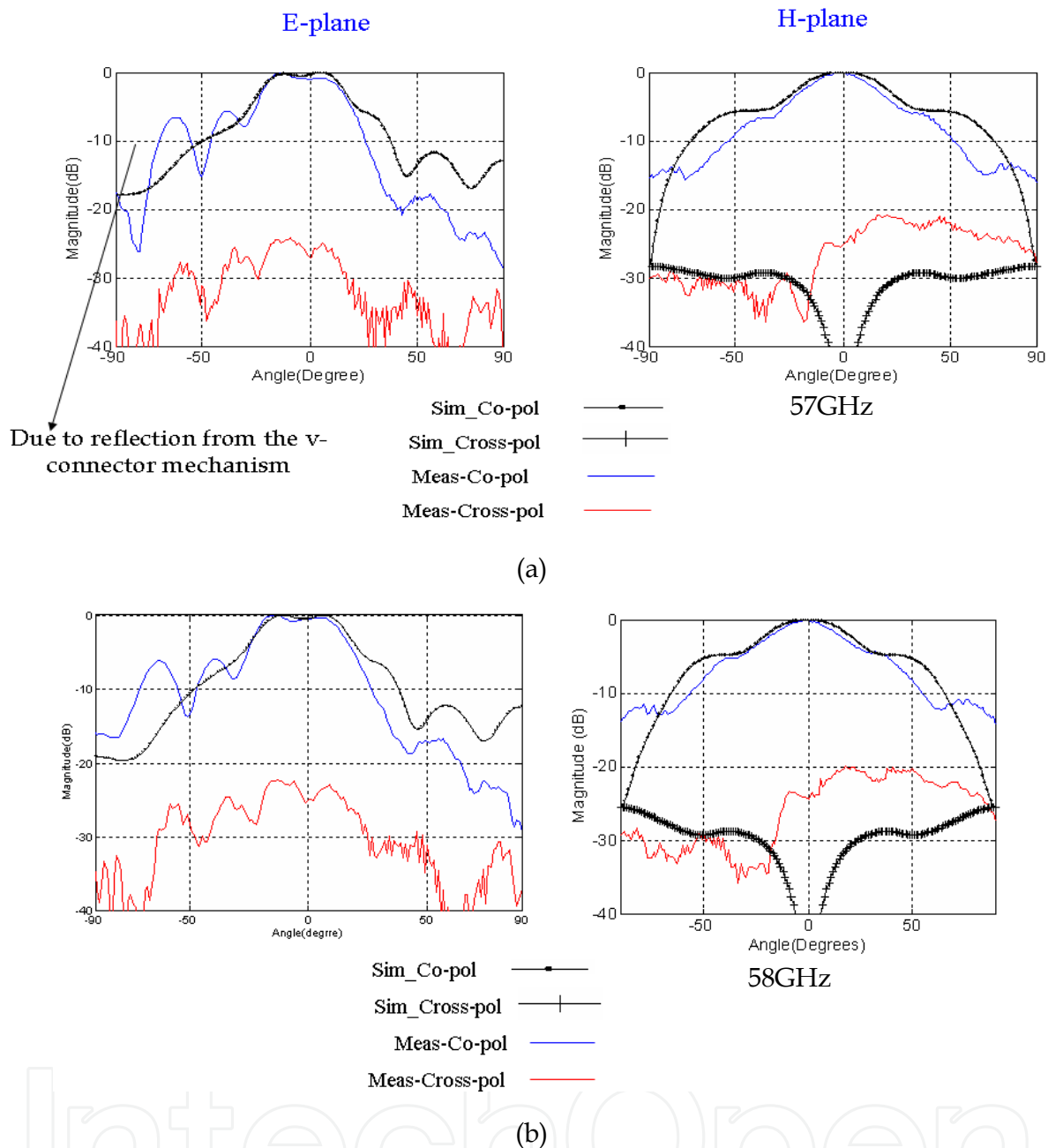


Fig. 5. Measured and simulated E-plane & H-plane radiation patterns of the parasitic patch Superstrate antenna (a) 57 GHz, (b) 58 GHz.

It is noted that for microstrip fed stacked patch antenna, the optimized superstrate size is  $1.1 \lambda_0$  for getting maximum gain and broad pattern. This value is considered as the limitation of size in this case. It is also observed from Fig. 3, that when the superstrate size is higher than  $1.1 \lambda_0$ , and when the height varies from  $0.5 \lambda_0$  to  $0.7 \lambda_0$  the broad nature of the gain decreases and starts coming down at 60 GHz .I.e. the pattern changes from broadside to sectorial and then to conical for different frequencies in the band as shown in Fig. 6 (for a superstrate size of  $2 \lambda_0$  &  $h_2=0.6 \lambda_0$ ), which may suitable for some other application (Vettikalladi et al., 2009b). Here, the small superstrate size is due to the presence of the parasitic patch that disturbs the field in the cavity (thickness =  $0.6 \lambda_0$ ).

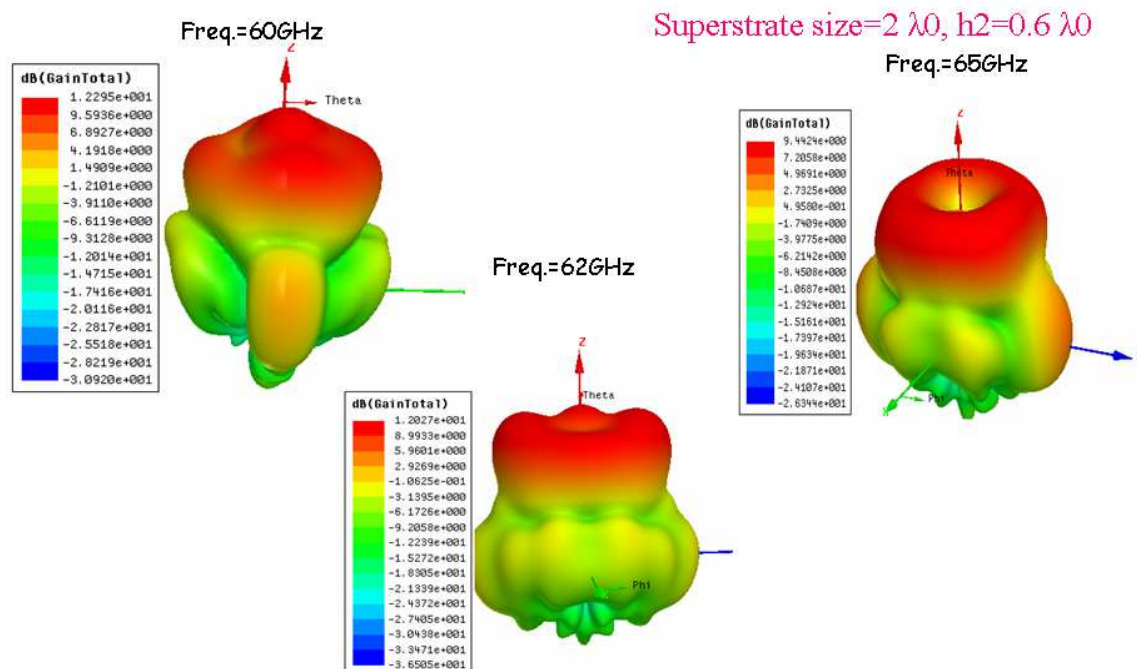


Fig. 6. Gain pattern for a microstrip fed parasitic patch superstrate with a superstrate size =  $2\lambda_0$ , for different frequencies in the band.

Since this kind of prototype is very difficult to manufacture and hence we are going to discuss with other kind of technology.

## 2.2 Slot coupled superstrate antenna

In this section, we are explaining a superstrate antenna with aperture coupled source as the excitation. We are also showing the importance of the size of the superstrate for getting maximum gain and also for getting consistent radiation pattern all over the frequency range of interest. Fig.7 shows the side view and the 3D view of a slot coupled patch antenna with superstrate. The slot is optimised to  $0.2\text{ mm} \times 1\text{ mm}$  for maximum coupling with a stub length of  $0.75\text{ mm}$ . In order to consider the easiness of implementation; we used a thick ground plane of thickness  $t=0.2\text{ mm}$ . The antenna consists of a patch with optimised dimension  $1.3\text{ mm} \times 1.3\text{ mm}$  on a substrate RT Duroid 5880 of permittivity 2.2 and a loss tangent  $\tan\delta = 0.003$  with a thickness  $t_1 = 0.127\text{ mm}$ . Low thickness and low permittivity substrate are used for reducing surface waves. A dielectric superstrate is added above the slot coupled patch antenna (Vettikalladi et al., 2009a). Here we used only one layer to avoid the technological manufacturing problems when many layers are used at 60 GHz. The material used for the superstrate is Roger substrate RT6006 with a relative permittivity of 7.5 at 60 GHz. Theoretically the thickness of superstrate must be  $\lambda_g/4$  ( $0.456\text{ mm}$ ), but here we took the thickness ( $t_2 = 0.635\text{ mm}$ ) close to the theoretical thickness available in market for good antenna performance. The distance between the superstrate and ground plane is  $0.5\lambda_0$  as per the theory (Gupta & Kumar, 2005). A Rohacell foam layer of permittivity 1.05 is sandwiched between base antenna and superstrate to fix all the layers.



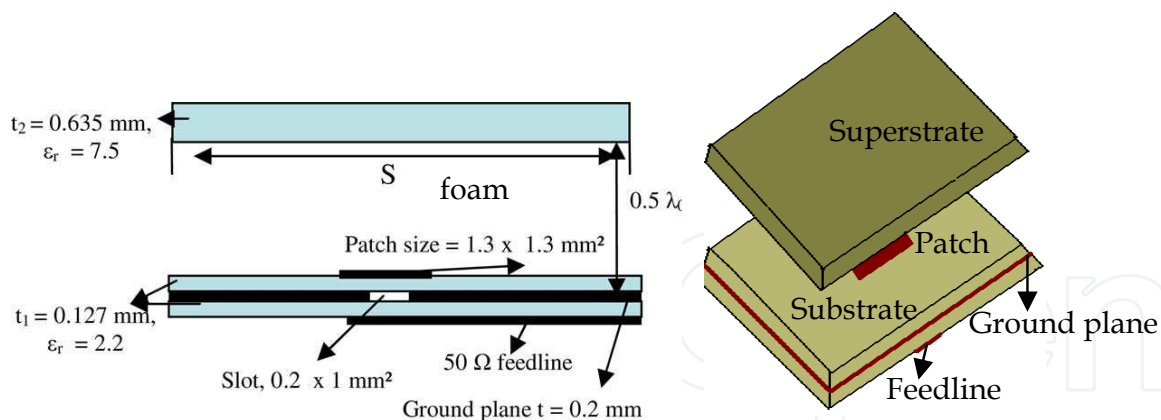


Fig. 7. Cutting plane and 3D view of aperture coupled antenna with superstrate, ground plane size =  $30 \times 30$  mm<sup>2</sup>.

Usually in all the known superstrate antennas large superstrates are used for improving the gain which not only increases the size of the antenna but also decreases the S11 bandwidth. But our objective is different, we want to use a small superstrate for obtaining high stable gain and constant radiation pattern all over the frequency band of interest. To study the effect of superstrate size 'S' and hence to optimize, we considered four square sizes ( $1 \lambda_0$ ,  $2 \lambda_0$ ,  $4 \lambda_0$  and  $6 \lambda_0$ ). Simulations are done using CST Microwave studio®. Fig. 8 shows the CST results of S11 and gain variations of the slot coupled antenna without superstrate and with varying superstrate size. It is observed that the S11 and gain vary with various size of the superstrate. When there is no superstrate, the antenna radiates at 60 GHz with a bandwidth of 3.7% over a frequency range of 58.9 to 61.1 GHz with a maximum gain of 5.9 dBi. It is noted that with superstrate the gain is highest for a superstrate size of  $2 \lambda_0$ . The 2:1 VSWR bandwidth is noted to be BW = 58.7 - 62.7 GHz i.e. 6.7% with a maximum gain of 14.9 dBi. It is also noticed that the gain decreases when the size of the superstrate is above or below  $2 \lambda_0$ .

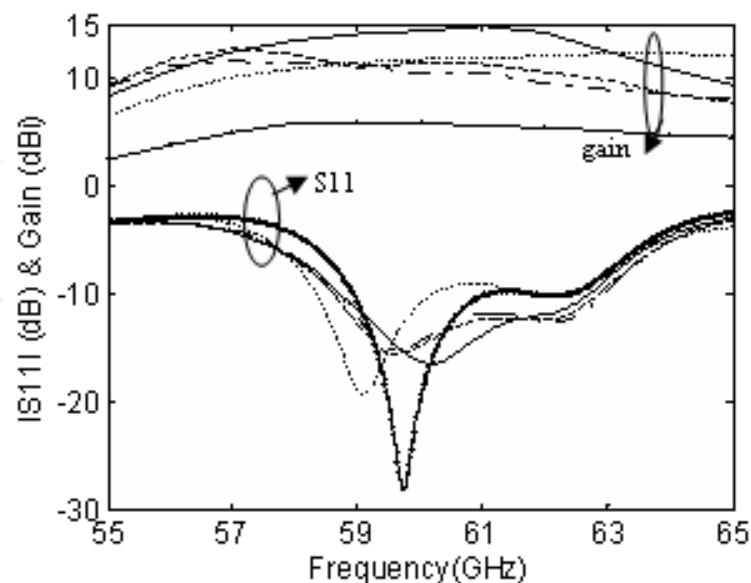


Fig. 8. Variation of S11 and gain without superstrate and with various superstrate dimensions. without superstrate —●—  $1 \lambda_0$  .....  $2 \lambda_0$  — — —  $4 \lambda_0$  - - - -  $6 \lambda_0$  - · - · - .

There is a gain enhancement of 9 dB with the superstrate. Fig. 9 shows the comparison of measured and simulated S11 and gain for the optimised superstrate size of  $2\lambda_0$ . Table II gives the comparison of measured and simulated S11 and gain for the optimised superstrate size. It is noted in S11 that there is a frequency band shift of 2.8% (1.7 GHz), when a V-connector is used and a frequency band shift of 1.5% when a V-band test fixture is used. These frequency shifts are maybe due to the combined effect of connectors and the inaccuracy of the distance between patch and superstrate for the experimental prototype.

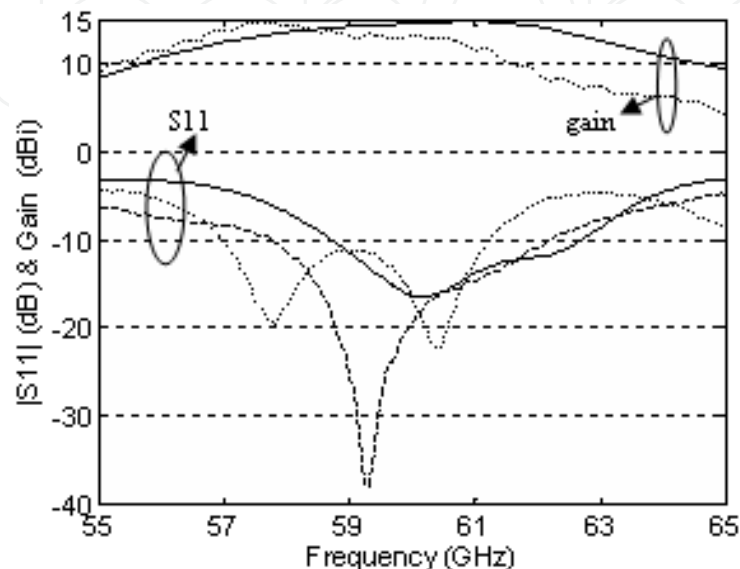


Fig. 9. Variation of S11 and gain with a superstrate dimension of  $2\lambda_0$ . Simulation — ; measured with V coaxial mounting connector - - - ; measured with V test fixture - . . .

Return loss bandwidth (simulated)	Return loss bandwidth (measured)	Maximum Gain (simulated)	Maximum Gain (measured)	Efficiency Estimated $\eta$
58.7 - 62.7 GHz (6.7%)	57 - 61.1 GHz (6.8%)	14.9 dBi	14.6 dBi	76%

Table II. Comparison between simulated and measured results of aperture coupled superstrate antenna.

Also the gain measured and simulated are in good agreement but with a frequency shift as explained. The gain is measured using comparison technique with a standard horn of known gain. For calculating the efficiency, we compared the measured gain with the simulated directivity. The measured and simulated E plane radiation patterns are shown in Fig. 10a for the optimised superstrate dimension. It is clear from Fig. 9 that the measured S11 and gain are shifted; the measured gain is maximum between 57 to 59 GHz and simulated gain is from 59 to 61 GHz. Hence the radiation patterns are plotted by taking in account of this frequency shifting (e.g.; that is radiation pattern plotted is, 60 GHz simulation and 58 GHz measurement, and so on). It is noted that the radiation patterns are found to be broad and in good agreement with measurements, and there is a cross polar level of less than -28 dB at all frequencies. The radiation patterns are verified to be the same in all the frequencies in the band of interest. The measured half-power beam width is found to be  $23^\circ$  at 58 GHz. Also verified by simulation that the back radiation in this case is below -22 dB as compared to the antenna without superstrate (-12 dB).

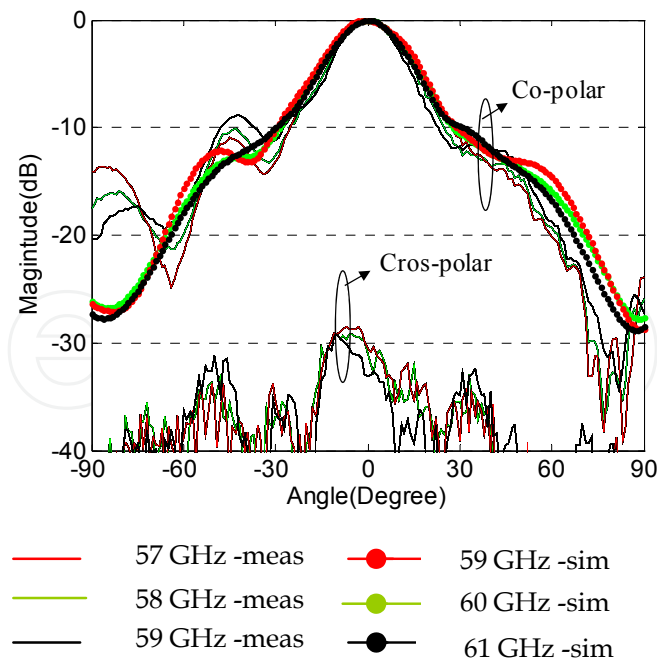


Fig. 10a. Measured and simulated E-plane radiation patterns of superstrate antenna.

The measured and simulated H plane radiation patterns are shown in Fig. 10b for the optimised superstrate dimension. The radiation patterns are also plotted by taking in account of shifting as explained in E plane radiation pattern. It is noted that the radiation patterns are found to be broad and in good agreement with measurements, and there is a cross polar level of less than -28 dB at all frequencies. The measured half-power beam width is found to be 22° at 58 GHz.

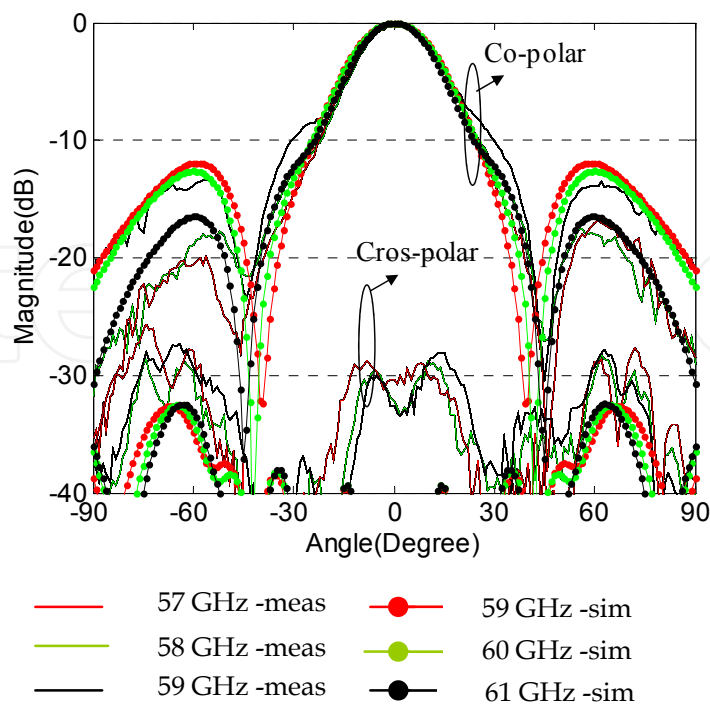


Fig. 10b. Measured and simulated H-plane radiation patterns of superstrate antenna.

When the superstrate size is higher than  $2\lambda_0$ , the broad nature of the pattern disappeared at 60 GHz. Fig. 11 shows the simulated (60 GHz) and measured (58 GHz) H plane radiation patterns of the antenna with a superstrate dimension of  $6\lambda_0$ . It is noted that the radiation patterns change from broad side to sectorial / null at 60 GHz, which is also useful for some other applications. It concludes that the dimension of the superstrate is critical for the optimum performance of the antenna. To conclude, the dimension of the superstrate is very important in order to get the consistent radiation pattern for the entire frequency band and it is found to be  $2\lambda_0$  in this case. This is the main difference from the already developed superstrate antennas published in the literature.

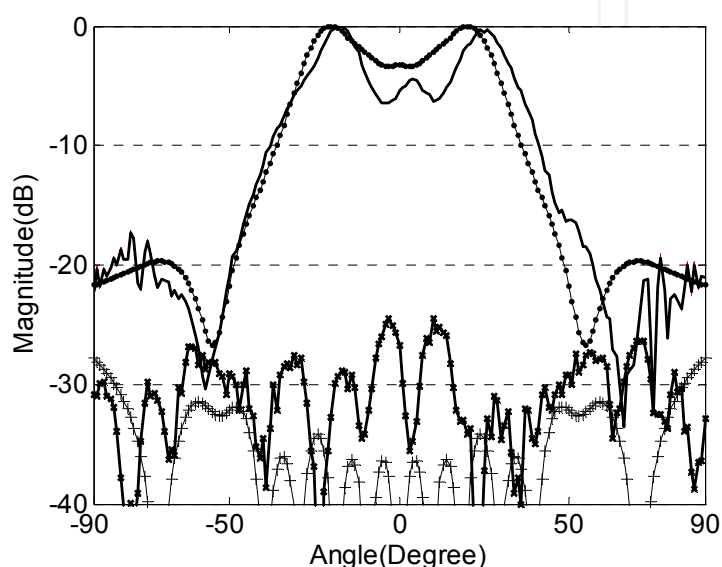


Fig. 11. Measured and simulated H-plane radiation pattern for a superstrate dimension of  $6\lambda_0$ . Co-simulated —○— Co-measured — — Cross-simulated —+— Cross-measured —×— .

### 2.2.1 Slot coupled 2x2 superstrate antenna array

Fig.12 (a) & (b) show the side view of an aperture coupled  $2 \times 2$  patch antenna array with superstrate and the feeding network. The distance between the elements in the array are optimized to be  $d = 1.3\lambda_0$  for obtaining maximum gain and to minimize coupling. All the base antenna parameters and substrate and superstrate are same as explained in section 2.2.

As explained in section 2.2, usually, large superstrates are used for improving the gain. But our objective is different: we want to use the smallest superstrate for obtaining high stable gain and consistent radiation pattern in the frequency band. To study the effect of superstrate size 'S' and hence to optimize it, here also we considered four square sizes ( $2.4\lambda_0$ ,  $3.2\lambda_0$ ,  $4\lambda_0$  and  $6\lambda_0$ ). Simulations are done using CST Microwave studio. Fig. 13 shows the CST results of S11 and directivity variations of the  $2 \times 2$  slot coupled antenna array with varying superstrate size. The S11 and directivity are affected by the size of the superstrate: the highest directivity of 18 dBi is obtained for a superstrate size of  $3.2\lambda_0$ . The resulting 2:1

VSWR bandwidth is 5% from 58.6 to 61.6 GHz. It is also noticed that the directivity decreases when the size of the superstrate is above or below  $3.2 \lambda_0$  and hence the optimised size of the  $2 \times 2$  superstrate antenna array is  $3.2 \lambda_0 \times 3.2 \lambda_0$ . Fig. 14 shows the comparison of measured and simulated S11, and measured gain with simulated directivity for the optimised superstrate size of  $3.2 \lambda_0$ .

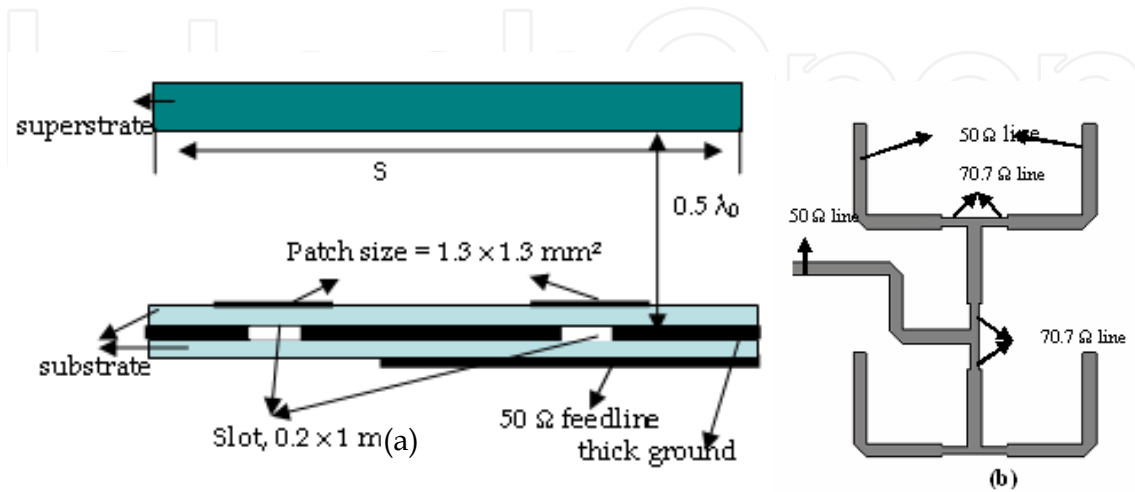


Fig. 12. a) Cutting plane of an aperture coupled  $2 \times 2$  antenna array with superstrate, ground plane size =  $6 \lambda_0 \times 10 \lambda_0$ , for connecting V band connector and for ease of measurement purpose, b)  $2 \times 2$  feeding network.

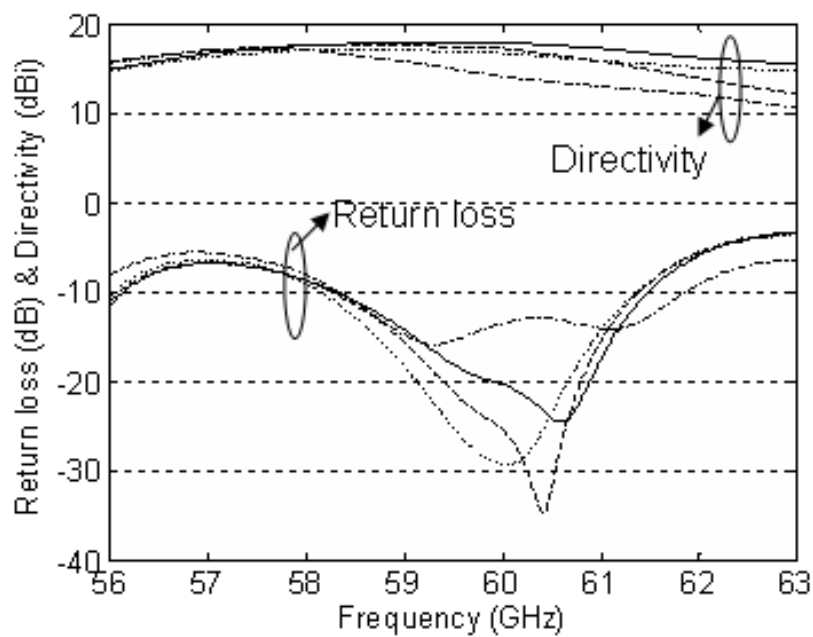


Fig. 13. Variation of return loss and directivity with various superstrate dimensions.  $2.4 \lambda_0$  .....  $3.2 \lambda_0$  —  $4 \lambda_0$  - - - -  $6 \lambda_0$  - · - · - .

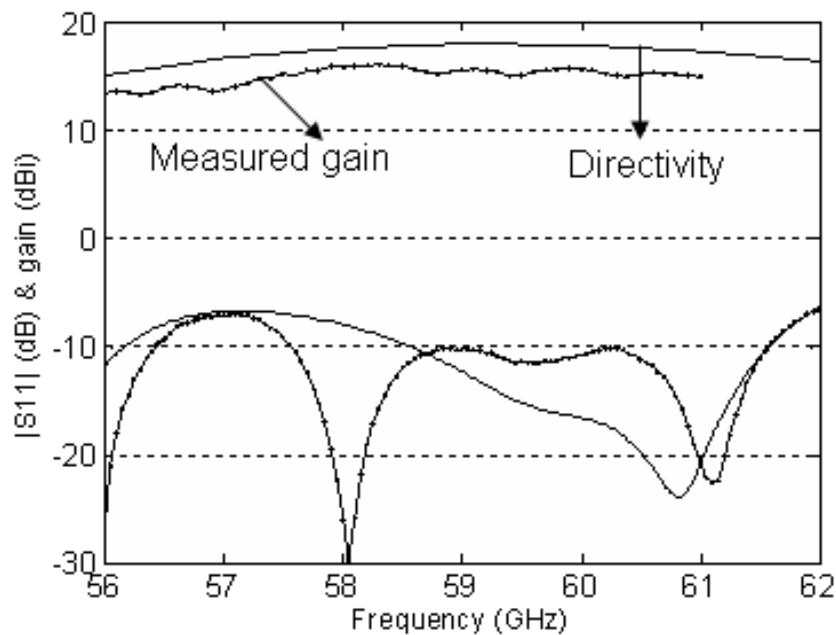


Fig. 14. Variation of S11 and gain with a superstrate dimension of  $3.2 \lambda_0$ .  
Simulation ——— measured —•— .

Table III gives the comparison of measured and simulated results for the optimised superstrate size (Vettikalladi et al., 2010a). It is found that the measured maximum gain is 16 dBi with S11 bandwidth of 6.7% and an estimated efficiency of 63%. With superstrate there is a gain enhancement of 4 dB compared to the classical  $2 \times 2$  array (Liu et al., 2009, Book chapter 5, O. Lafond & M. Himdi). The measured gain is maximum at 58 GHz while the simulated directivity is maximum at 59 GHz, which corresponds to 1.7% frequency shift.

Return loss bandwidth (simulated)	Return loss bandwidth (measured)	Maximum Directivity (simulated)	Maximum Gain (measured)	Efficiency Estimated $\eta$
58.6 - 61.6 GHz (5%)	57.6 - 61.6 GHz (6.7%)	18 dBi	16 dBi	63%

Table III. Comparison of simulated and measured  $2 \times 2$  superstrate antenna array.

The simulated and measured E-plane radiation patterns are shown in Fig. 15 for the optimised superstrate dimensions. It is clear from Fig. 14 that the measured gain is maximum between 58 to 59 GHz and simulated is from 59 to 60 GHz. Hence the radiation patterns are plotted by taking in account of this 1.7% shift (e.g. ; that is radiation pattern plotted is, 60 GHz simulation and 59 GHz measurement, etc). It is noted that the radiation patterns are found to be broad and in good agreement with measurements. The measured half-power beam width (HPBW) is found to be  $17^\circ$  at 59 GHz.

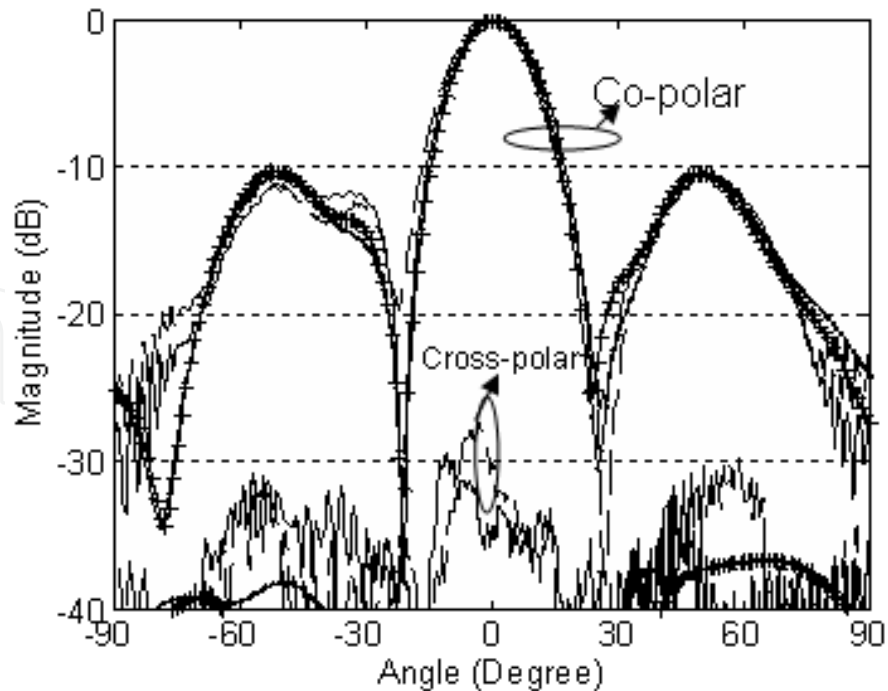


Fig. 15. Measured and simulated E-plane radiation patterns of  $2 \times 2$  superstrate antenna array.  
 58 GHz - measured — — — 59 GHz - simulated —•—  
 59 GHz - measured ——— 60 GHz - simulated —+—.

The measured and simulated H-plane radiation patterns are shown in Fig. 16 for the optimised superstrate dimension. The radiation patterns are also plotted by taking into

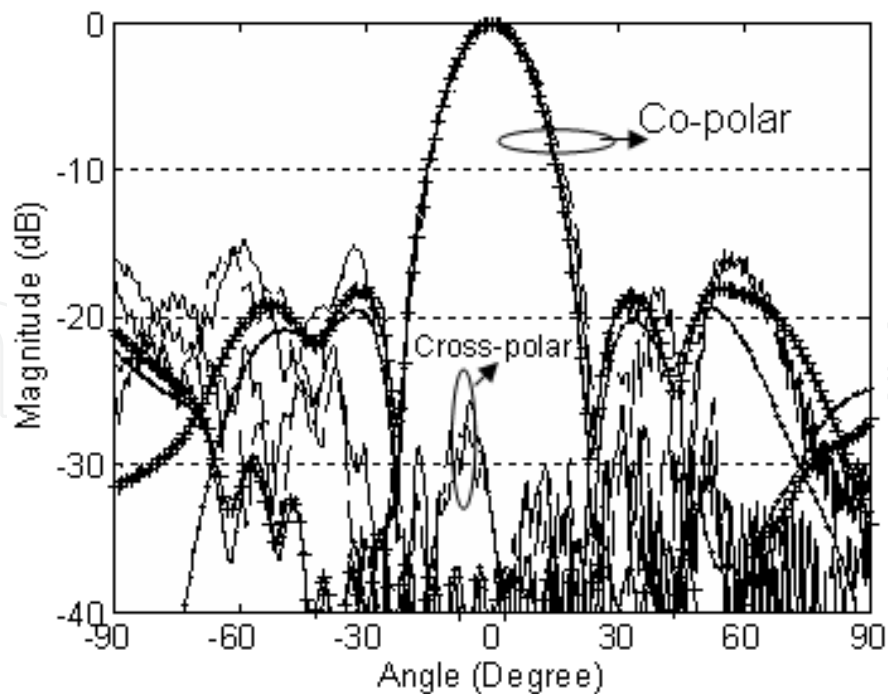


Fig. 16. Measured and simulated H-plane radiation patterns of  $2 \times 2$  superstrate antenna array.  
 58 GHz - measured ——— 59 GHz - simulated —+—  
 59 GHz - measured — — — 60 GHz - simulated —•—.

account the shift as explained for E-plane radiation patterns. It is noted that the radiation patterns are found to be broad and in good agreement with measurements. The measured HPBW is found to be  $16^\circ$  at 59 GHz. The cross polarisation level is lower than -26 dB on both the E and H-plane, and is lower than -19 dB at  $45^\circ$  cut plane in 3D pattern.

### 2.2.2 Slot coupled 4x4 superstrate antenna array

Fig. 17 shows the photograph of a 4 x 4 array antenna array with superstrate. The antenna parameters and the distance between the elements are the same as explained for 2 x 2 superstrate antenna array in Section 2.2. The same substrate for the superstrate is used. Here also the superstrate should be optimised and it is found to be  $6 \lambda_0 \times 6 \lambda_0$  which is the total size of the antenna. For manufacturing this prototype, because of the 4x4 array, two metal wedges of 3 mm width are used to position the superstrate at 2.3 mm ( $\sim \lambda_0/2 - 0.127$  mm) above the patch array. This mechanical solution is found to be better in this case than foam due to the relation between superstrate position sensitivity and gain increase.

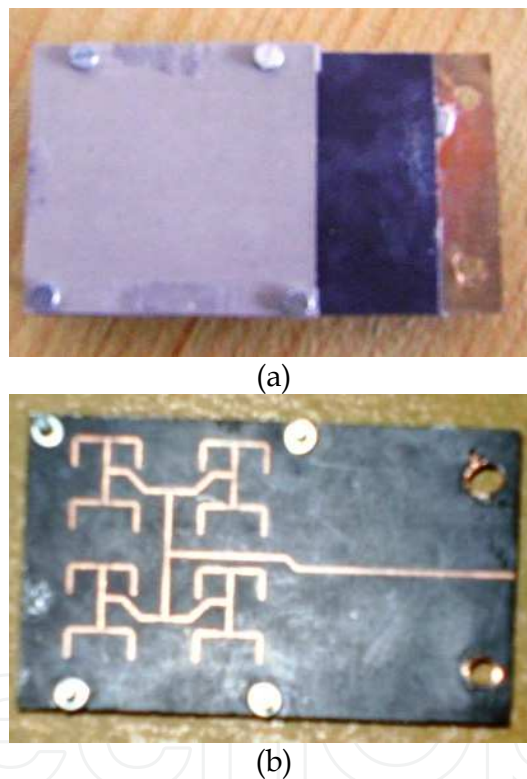


Fig. 17. Photograph of 4 x 4 superstrate antenna array prototype (a) Top view of superstrate antenna (b) view of antenna feed line network from bottom side. Ground plane taken is  $6 \lambda_0 \times 10 \lambda_0$ , for connecting V band connector and for ease of measurement purpose.

Fig. 18 shows the measured and simulated S11, and measured gain with simulated directivity. It is found that the maximum gain measured is 19.7 dBi with an efficiency of 51% (simulated directivity = 22.6 dBi) which is far better than a classical 6 x 6 array antenna of gain 17.5 dBi with an efficiency of 40% at 59 GHz (Lafond et al. 2001), and an 8 x 8 array antenna (size =  $6.5 \lambda_0 \times 6.5 \lambda_0$ ) of gain 19.7 dBi with an efficiency of  $\sim 40\%$  as explained in (Nesic et al., 2001). The S11 bandwidth measured for the 4 x 4 superstrate antenna array is 57.9 GHz to 61.3 GHz (5.7%).



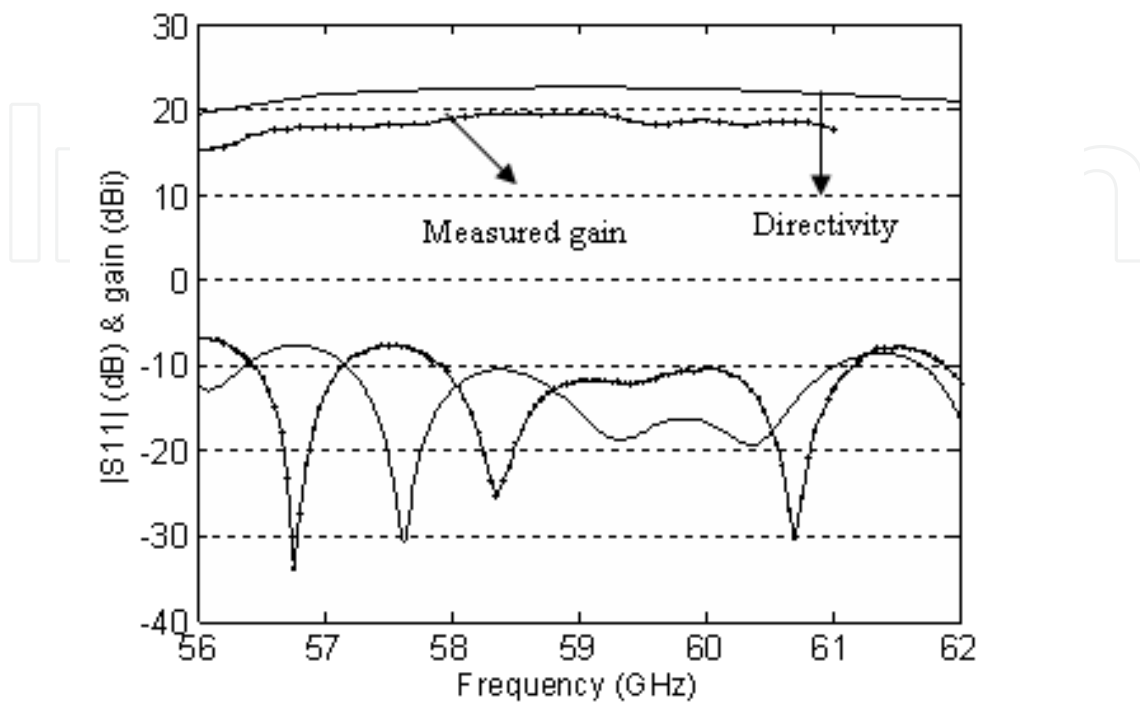


Fig. 18. Variation of S11 and gain with a square superstrate dimension of  $6 \lambda_0$ . Simulation ——— measured —•—.

It is clear from Fig. 18 that the gain measured and simulated are maximum from 58 GHz to 60 GHz. The simulated and measured H-plane radiation patterns are shown in Fig. 19 (a). It is noted that the simulated patterns are in good agreement with the measured results. The measured HPBW is  $8^\circ$  at 60 GHz.

The measured and simulated E-plane radiation patterns are shown in Fig. 19(b) for the optimised superstrate dimension. The radiation patterns are broad and the agreement between measurement and simulation are quite acceptable. The measured HPBW is found to be  $10^\circ$  at 60 GHz. In this case, the cross polarization level is lower than -25 dB on both the E and H-plane, and is lower than -16 dB at  $45^\circ$  cut plane in 3D pattern.

For both the presented antennas, a distance between the elements of  $1.3 \lambda_0$  is used for the source array, which induces high ambiguity side lobes for both cases when there is no superstrate: -2 dB for a  $2 \times 2$  array and -1.9 dB for  $4 \times 4$  array as shown in Fig. 20. Adding a superstrate will strengthen the main lobe while suppressing the ambiguity side lobes to less than -10 dB for both the arrays without affecting the back radiation as shown in Fig. 20. It also strengthens the front to back ratio as shown in the figure. It is to be underlined that the size of the superstrate is a key point of the design of such structures. In fact the nature of the pattern is conditioned by the choice of this parameter: a broad pattern is obtained for a size limited to  $3.2 \lambda_0 \times 3.2 \lambda_0$  for  $2 \times 2$  array and  $6 \lambda_0 \times 6 \lambda_0$  for  $4 \times 4$  arrays.

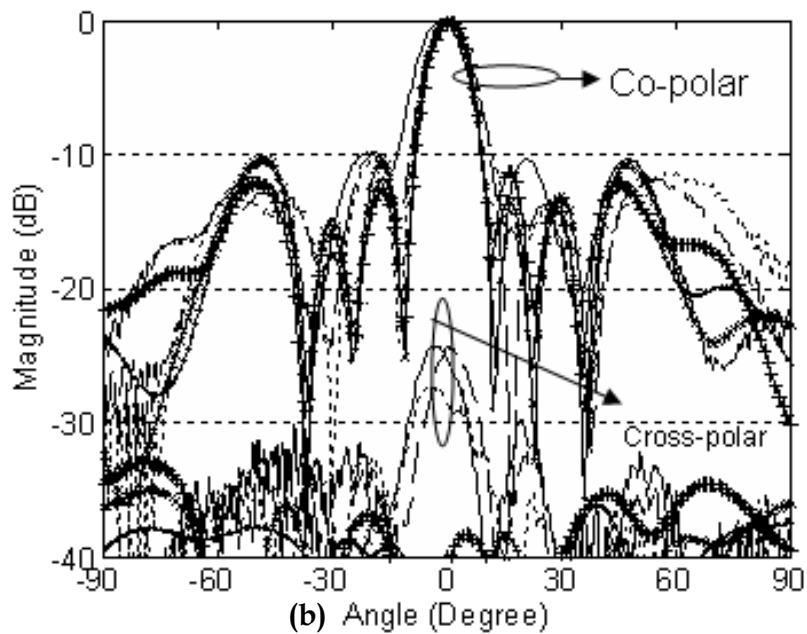
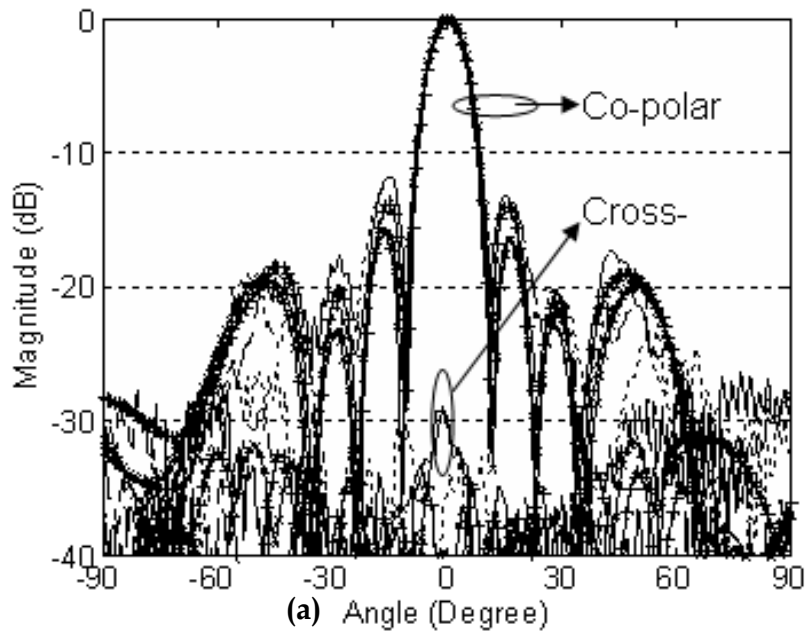


Fig. 19. Measured and simulated (a) H plane & (b) E plane radiation patterns of 4 x 4 superstrate antenna array.

58 GHz - measured ..... 58 GHz - simulated —X—  
 59 GHz - measured - - - - 59 GHz - simulated —•—  
 60 GHz - measured ——— 60 GHz - simulated —+—

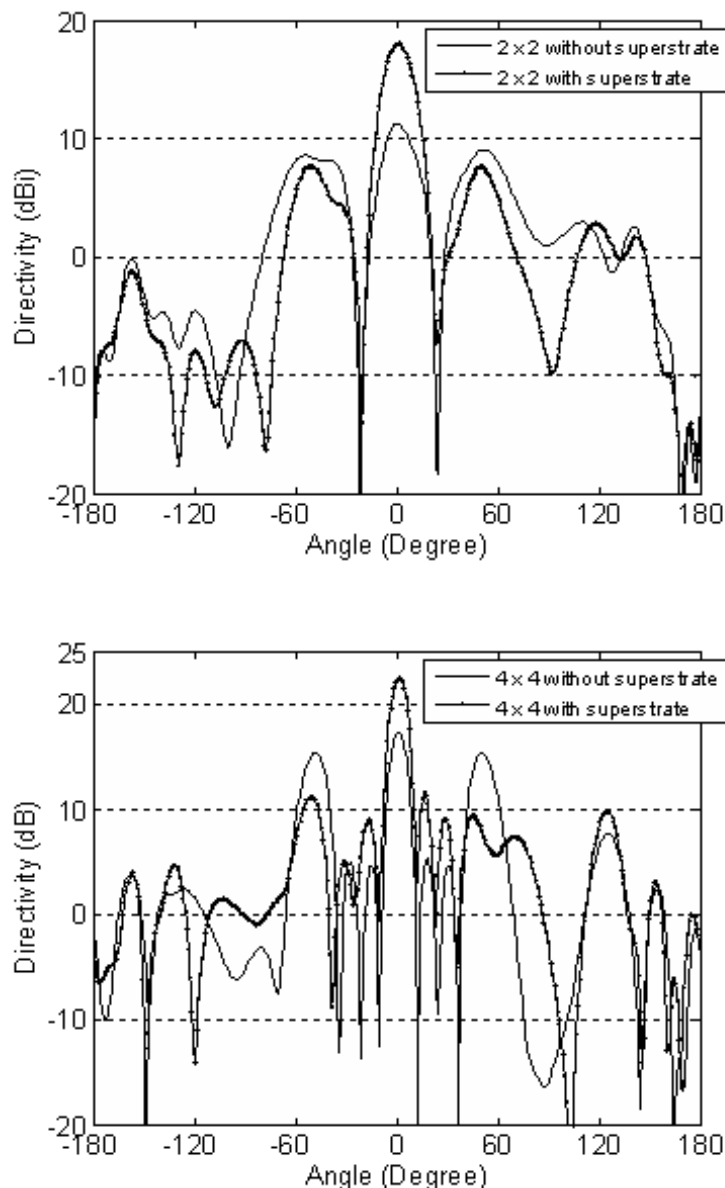


Fig. 20. Comparison of simulated results of  $2 \times 2$  and  $4 \times 4$  arrays without and with superstrate in terms of main beam, side lobe and back radiation.

### 2.3 Superstrate aperture antenna

In this section we are using another source, as aperture, for exciting the antenna. The side view of an aperture antenna with superstrate is shown in Fig. 21(a). The aperture is optimised to  $4.4 \text{ mm} \times 1 \text{ mm}$  for maximum coupling with a stub length of  $0.4 \text{ mm}$  (Fig. 21(b)). To improve the rigidity of antenna, a ground plane of thickness  $t = 0.2 \text{ mm}$  is used. For maintaining the exact air thickness in practical prototype, the superstrate is inserted within an air pocket realized in a Rohacell foam block of permittivity 1.05, as shown in Fig. 21(c). All the substrate and superstrate material used are the same as explained in section 2.2.

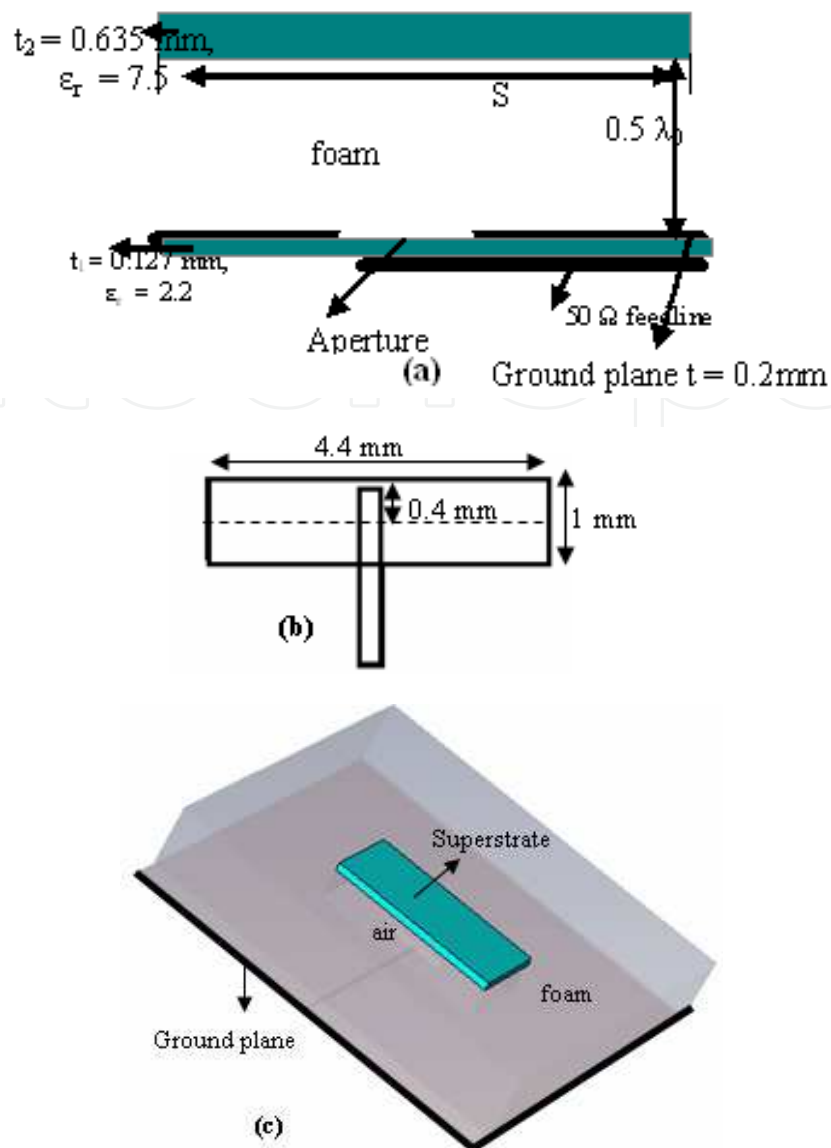


Fig. 21. (a) Cutting plane of aperture antenna with superstrate, ground plane size =  $6 \lambda_0 \times 6 \lambda_0$ . (b) Aperture and stub in details. (c) Overview of the Prototype: Details of the superstrate and air gap within foam.

In this case also we want to study the effect of superstrate size on antenna performance. To study the effect of superstrate size 'S' and hence to optimize it, a parametric study has been performed, using commercial electromagnetic software CST Microwave studio. To highlight the effects of this parameter, results obtained for four sizes ( $1 \lambda_0 \times 2 \lambda_0$ ,  $2 \lambda_0 \times 2 \lambda_0$ ,  $1.2 \lambda_0 \times 2.7 \lambda_0$  and  $3 \lambda_0 \times 3 \lambda_0$ ) are reported in Fig. 22. It is observed that both the S11 and the directivity vary according to the size of the superstrate. A maximum directivity of 14.5 dBi is obtained for a superstrate size of  $1.2 \lambda_0 \times 2.7 \lambda_0$ . The corresponding 2:1 VSWR bandwidth is noted to be equal to 57.5 - 71 GHz i.e. 22.5%. It is also noticed that the directivity decreases when the size of the superstrate is above or below this optimized value. We plotted directivity only up to 65 GHz because of the decline in the values after that. When the superstrate size is higher than the optimized value, then there is a plunge in directivity as shown in Fig. 22. Hence the broad nature of the pattern moved out at 60 GHz as explained

in (Vettikalladi et al., 2009a), i.e the radiation patterns change from broad side to sectorial / null at 60 GHz, which is also useful for some other applications.

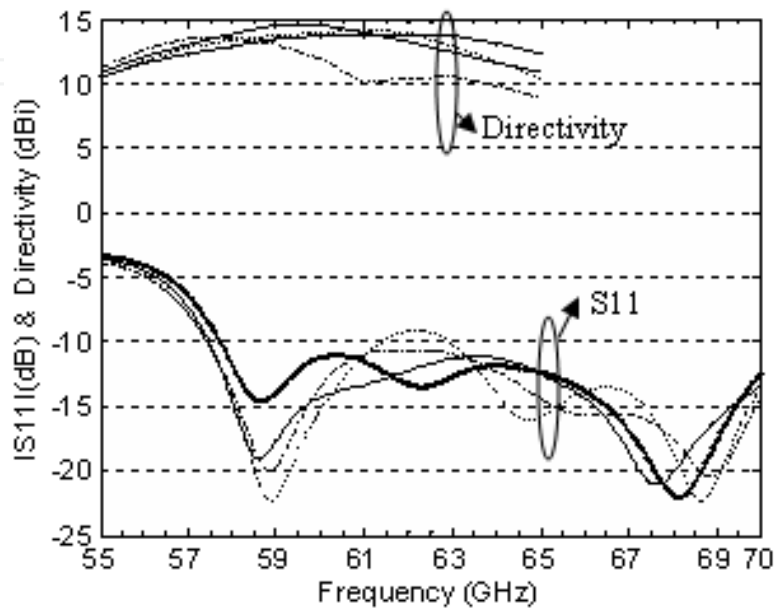
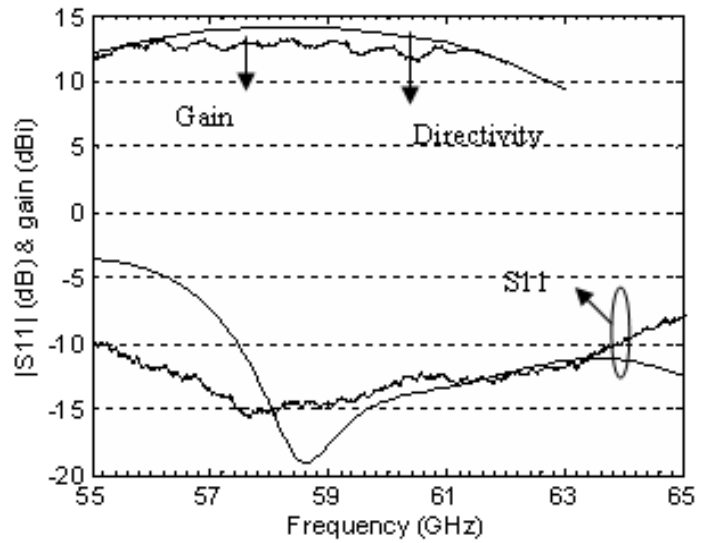
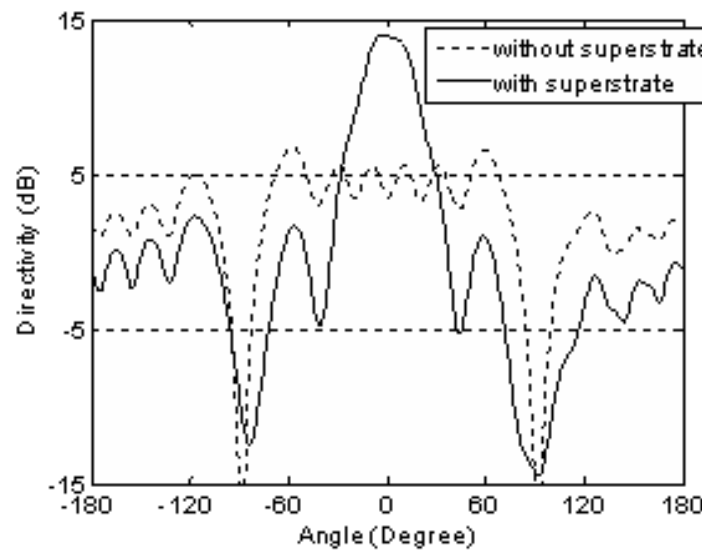


Fig. 22. Simulated results of S11 and directivity with various superstrate dimensions.  $1 \lambda_0 \times 2 \lambda_0$  —●— ;  $2 \lambda_0 \times 2 \lambda_0$  ..... ;  $1.2 \lambda_0 \times 2.7 \lambda_0$  —●— ;  $3 \lambda_0 \times 3 \lambda_0$  - - - - .

It concludes that in this case the dimension of the superstrate is critical for the optimum performance of the antenna. Also we can control the shape of the pattern by changing the dimension of the superstrate from broadside to sectorial / null. The comparison of measured and simulated S11, and measured gain with simulated directivity for the optimized superstrate size is shown in Fig. 23 (a). Table IV gives the summary of these results (Vettikalladi et al., 2010b). It is noted that the measured 2:1 VSWR bandwidth is 15% which is larger compared to the superstrate slot coupled antenna (Vettikalladi et al., 2009a), where the bandwidth was only 6.8%. The gain is measured using comparison technique with a standard gain horn. It is found to be 13.1 dBi. Moreover, it is almost flat (ripple  $\sim 0.5$  dB) over a bandwidth of 5 GHz. To determine the efficiency, we compared the measured gain with the simulated directivity. The estimated efficiency is 79%. In order to highlight the effect of the superstrate for this configuration, the simulated comparison of E-plane radiation pattern of aperture antenna with superstrate and without superstrate is shown in Fig. 23 (b). The ripples in the pattern without superstrate are due to the diffraction from the edges of the limited ground plane. Also it is clear that aperture antenna is a bidirectional antenna, superstrate technology make this antenna to unidirectional without adding any reflector, which is a highlight of the superstrate with this kind of source. I.e. Superstrate makes the antenna pattern directive and there is a gain enhancement of 8 dB compared to its basic aperture antenna.



(a)



(b)

Fig. 23. (a) Results of S11 and gain with a superstrate dimension of  $1.2 \lambda_0 \times 2.7 \lambda_0$ . Simulation —•—; measurement —. (b) Simulated comparison of E-plane antenna radiation pattern with and without superstrate.

The measured and simulated H- and E-plane radiation patterns at 57 GHz, 60 GHz and 62 GHz are shown in Fig. 24 for the optimized superstrate dimension. It is noted that the radiation patterns are found to be broad and in agreement with simulations. The cross polar level is less than -25 dB for H-plane and -20 dB for E-plane respectively, for all the frequencies in the band. The measured half-power beam widths (HPBW) at 60 GHz are  $26^\circ$  for H-plane and  $30^\circ$  for E-plane respectively. The measured cross polarization level is lower than -17 dB at  $45^\circ$  cut plane in 3D patterns of both planes.

Return loss bandwidth (simulated)	Return loss bandwidth (measured)	Maximum Directivity of the prototype (simulated)	Maximum Gain (measured)	Efficiency Estimated $\eta$
57.5-71 GHz (22.5%)	55 - 64GHz (15%)	14.1 dBi	13.1 dBi	79%

Table IV. Comparison between simulated and measured results superstrate aperture antenna.

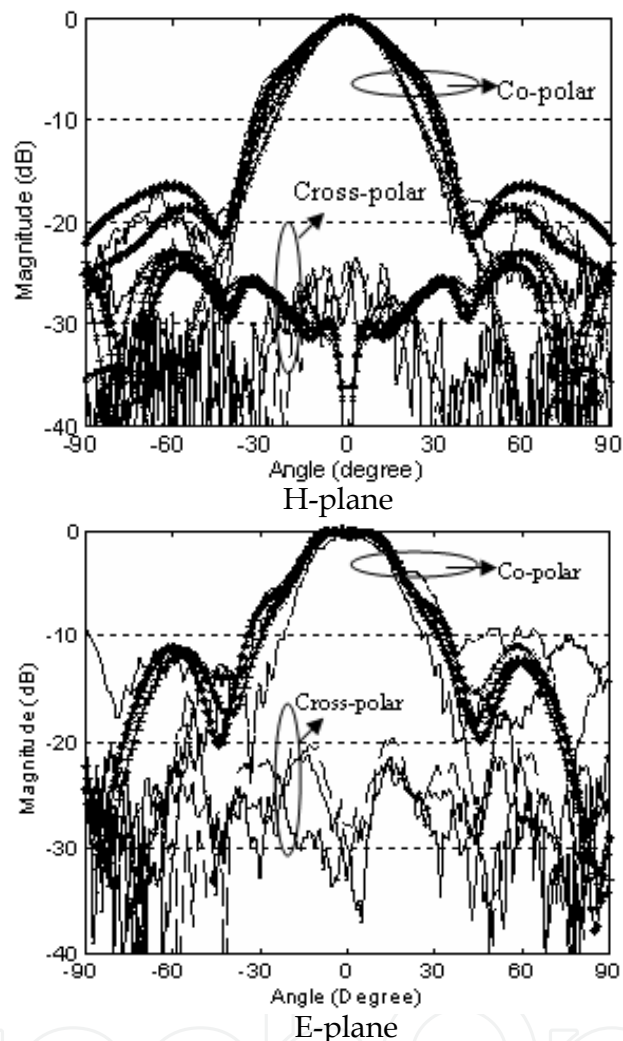


Fig. 24. Measured and simulated H-plane &amp; E- plane radiation patterns of superstrate antenna (Co and Cross polarisation).

57 GHz -Simulated  $\times$  ; 57 GHz - Measured  $\bullet$  ;  
 60 GHz -Simulated  $+$  ; 60 GHz -Measured  $\text{—}$  ;  
 62 GHz - Simulated  $\ast$  ; 62 GHz - Measured  $\text{---}$  .

### 2.3.1 2x2 superstrate aperture antenna array

The side and 3D view of a 2 x 2 aperture antenna array with superstrate are shown in Figs. 25(a) and (c). All the parameters of the antenna are the same as explained in section 2.3. For maintaining the exact air thickness, the superstrate is inserted within an air pocket realized in Rohacell foam as shown in Fig. 25(c). The distance between the elements in the array is optimized as  $d = 1.3 \lambda_0$  for obtaining maximum gain and to minimize coupling. The 2 x 2 feeding network is exposed in Fig. 25(b). In a classical array (without superstrate), when the

distance between the patches is  $d = 1.3 \lambda_0$ , high ambiguity side lobes appear with almost the same level as the main lobe. Adding a superstrate strengthens the main lobe while reducing the ambiguity side lobes to less than -10 dB (E-plane) as shown in Fig. 26. It also strengthens the front to back ratio as shown in the figure. It has to be underlined that the size of the superstrate is a key point for the design of such structures as explained in previous cases.

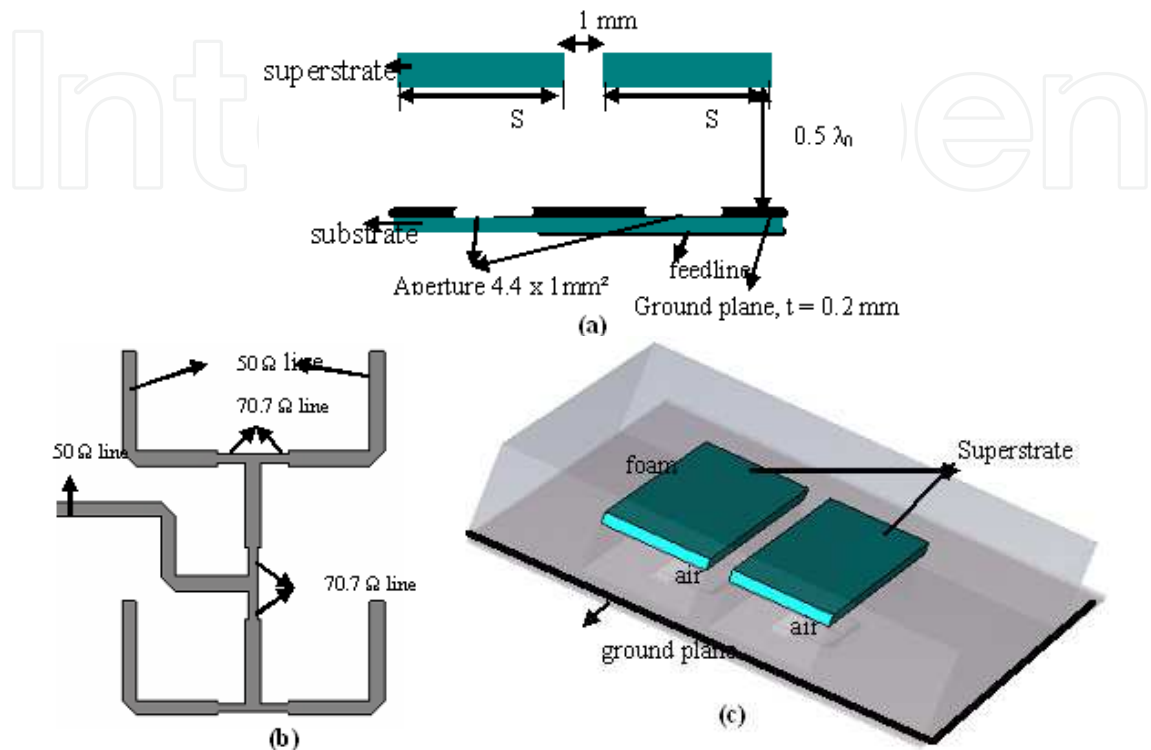


Fig. 25. (a) Cutting plane of a  $2 \times 2$  aperture antenna array with superstrate, ground plane size =  $6 \lambda_0 \times 10 \lambda_0$  for connecting V band connector and for ease of measurement purpose. (b)  $2 \times 2$  feed network. (c) Overview of  $2 \times 2$  array prototype: details of the two separate superstrate sheets and air gap within foam.

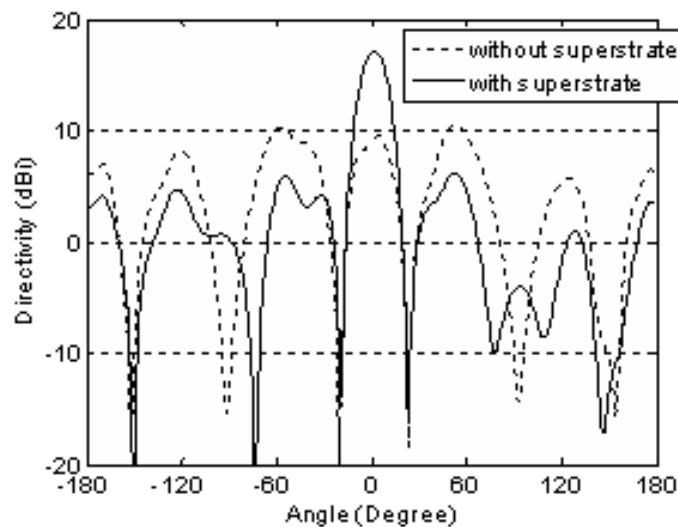


Fig. 26. Simulated comparison of  $2 \times 2$  antenna array pattern ( $d = 1.3 \lambda_0$ ) with and without superstrate (E-plane).



As did in previous sections, we studied the effect of superstrate size 'S' by simulating different sizes and the optimized solution is found to be two pieces of dimension  $1.2 \lambda_0 \times 4 \lambda_0$ , one sheet for two aperture antenna, with a spacing of 1mm as shown in Fig. 25(b). If we use a single piece with a size of  $2.6 \lambda_0 \times 4 \lambda_0$ , then the gain is little lower than in the previous case. The comparison of measured and simulated S11, and measured gain with simulated directivity for the optimized superstrate size is shown in Fig. 27. The highest directivity of 17.9 dBi is obtained for the optimized superstrate size. The resulting simulated 2:1 VSWR bandwidth is 11.3% from 57.2 to 64 GHz.

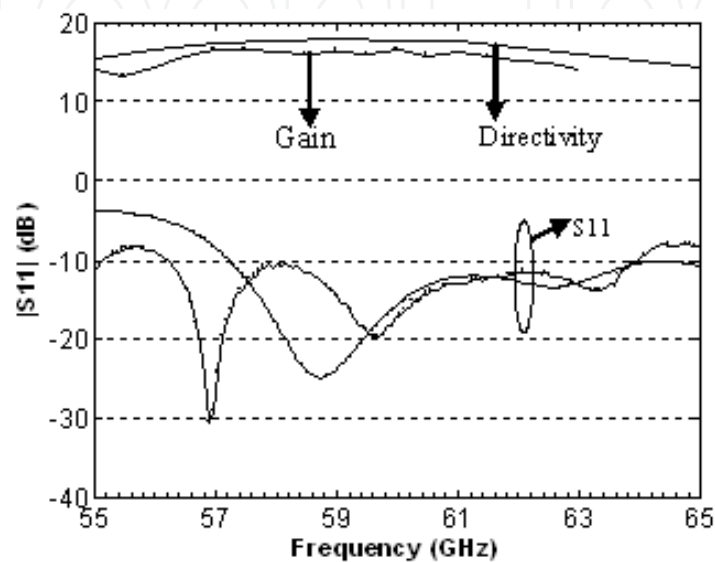


Fig. 27. Variation of S11 and gain for a  $2 \times 2$  superstrate aperture antenna array. Simulation —; measurement —•—.

Table V gives the comparison of measured and simulated results for the optimized superstrate size. It is found that the maximum measured gain is 16.6 dBi with S11 bandwidth of 13.3% (56 GHz - 64 GHz), and an estimated efficiency of 74%. This gain is comparable to a classical  $4 \times 4$  array at 60 GHz but with better efficiency (Lafond 2000). Also the measured gain is almost stable (ripple  $\sim 0.8$  dB) over 5 GHz (57 GHz - 62 GHz) in the band of interest (Vettikalladi et al., 2010c).

Return loss bandwidth (simulated)	Return loss bandwidth (measured)	Maximum Directivity (simulated)	Maximum Gain (measured)	Efficiency Estimated $\eta$
57.2 - 64 GHz (11.3%)	56 - 64 GHz (13.3%)	17.9 dBi	16.6 dBi	74%

Table V. Comparison between simulated and measured results of a  $2 \times 2$  superstrate aperture antenna array.

The measured and simulated H- and E-plane radiation patterns at 57 GHz, 60 GHz and 62 GHz are shown in Figs. 28 (a) & (b) respectively for the optimized superstrate dimension. It is noted that the radiation patterns are found to be broad and in good agreement with simulations. The measured cross polar levels are -26 dB for H-plane and -20 dB for E-plane respectively. The radiation patterns are verified to be the same in all the frequencies in the band of interest. The measured HPBWs are  $17^\circ$  for H-plane and  $16^\circ$  for E-plane respectively at 60 GHz.

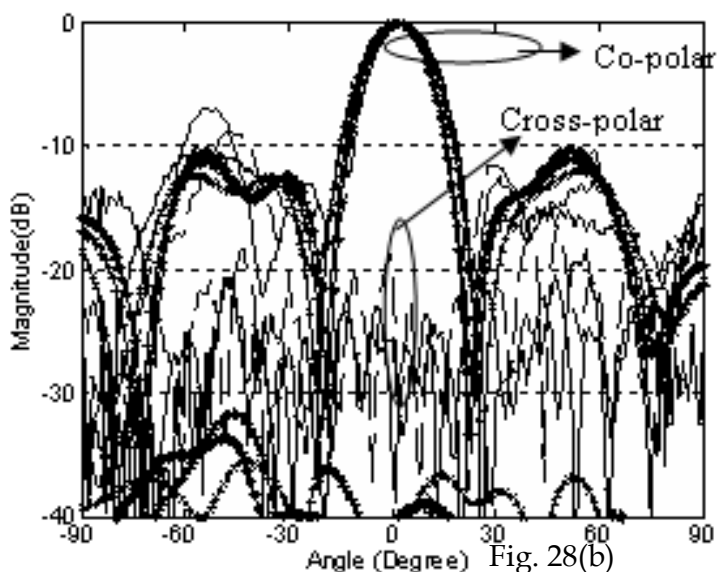
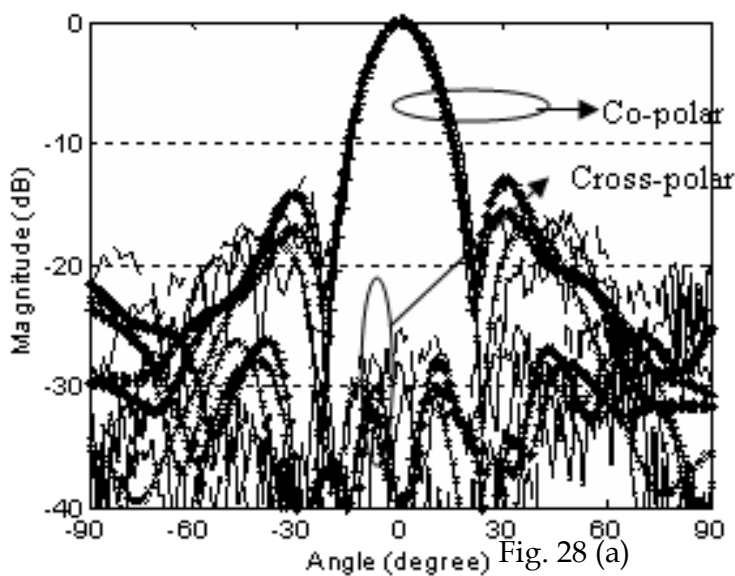


Fig. 28. Measured and simulated H-plane (a) & E-plane (b) radiation patterns of the 2 x 2 superstrate antenna array (Co and Cross polarisation).

57 GHz - Simulated —×— ; 57 GHz - Measured —●— ;  
 60 GHz - Simulated —+— ; 60 GHz - Measured ——— ;  
 62 GHz - Simulated —\*— ; 62 GHz - Measured - - - - .

### 2.3.2 16 x 16 superstrate aperture antenna array

Finally we developed a big array to obtain very high gain of nearly 30 dBi for 60 GHz outdoor communication, for example from one department to another department inside a university (< 1km). Fig. 29 (a) depicts the 3D side view of the 16 x 16 array prototype. The antenna parameters and the distance between the elements are all same as explained in Section 3.2. For maintaining the exact air thickness, the superstrate is inserted within an air

pocket realized in Rohacell foam as shown in Fig. 29(a). The 16 x 16 feeding network is showing in Fig. 29(b).

As pointed out in previous section, we want to use the smallest superstrate for obtaining high stable gain and consistent radiation pattern in the frequency band. We studied the effect of superstrate size 'S' by simulating different sizes and the optimized size is found to be 16 pieces of dimension  $1.2 \lambda_0 \times 21.8 \lambda_0$ , one sheet for 16 aperture antenna, with a spacing of 1mm as shown in Fig. 29(a). If we use a single piece with a size of  $20.6 \lambda_0 \times 21.8 \lambda_0$ , then the gain is little lower than in the previous case.

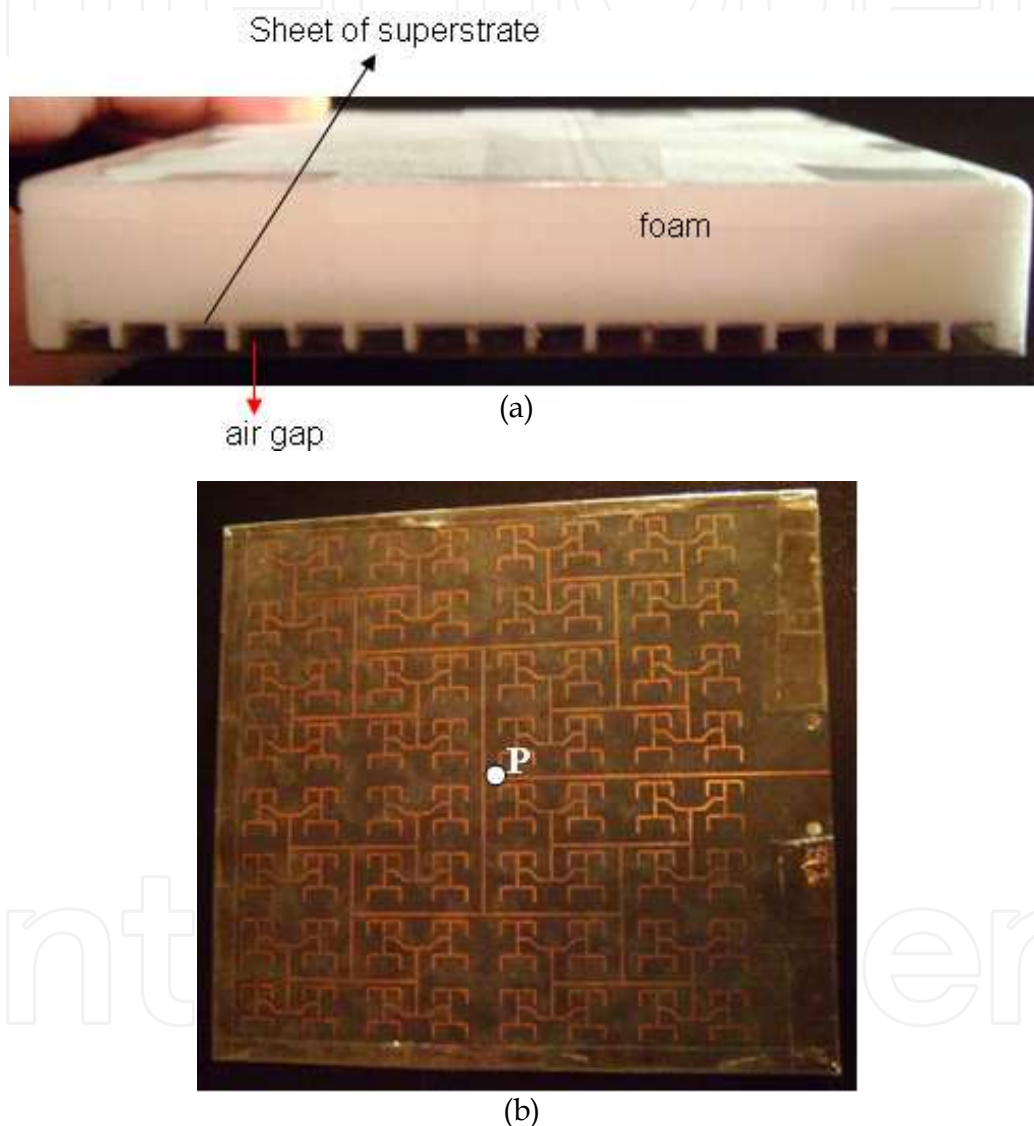


Fig. 29. (a) Side overview of 16 x 16 array prototype: details of the 16 separate superstrate sheets and air gap within foam, total size =  $20.6 \lambda_0 \times 21.8 \lambda_0$ . (b) 16 x 16 feed network.

The comparison of measured and simulated S11, and measured gain with simulated directivity for the optimised superstrate size is shown in Fig. 30. The highest simulated directivity of 33.3 dBi is obtained for the optimised superstrate size. The resulting simulated 2:1 VSWR bandwidth is 22 %. It is found that the maximum measured gain is 29.4 dBi ( at point 'P' in Fig. 29 (b)) with S11 bandwidth of 16.7 % (54 GHz - 64 GHz), and an estimated

efficiency of 41%. The measured and simulated E- and H-plane radiation patterns at 57 GHz, 60 GHz and 62 GHz are shown in Figs. 31(a) and (b) respectively for the optimised superstrate dimension. It is noted that the radiation patterns are found to be broad and in good agreement with simulations. The measured cross polar levels are -28 dB for H-plane and -26 dB for E-plane respectively. The radiation patterns are verified to be the same in all the frequencies in the band of interest. The measured HPBW's are 2.5° for H-plane and E-plane respectively at 60 GHz.

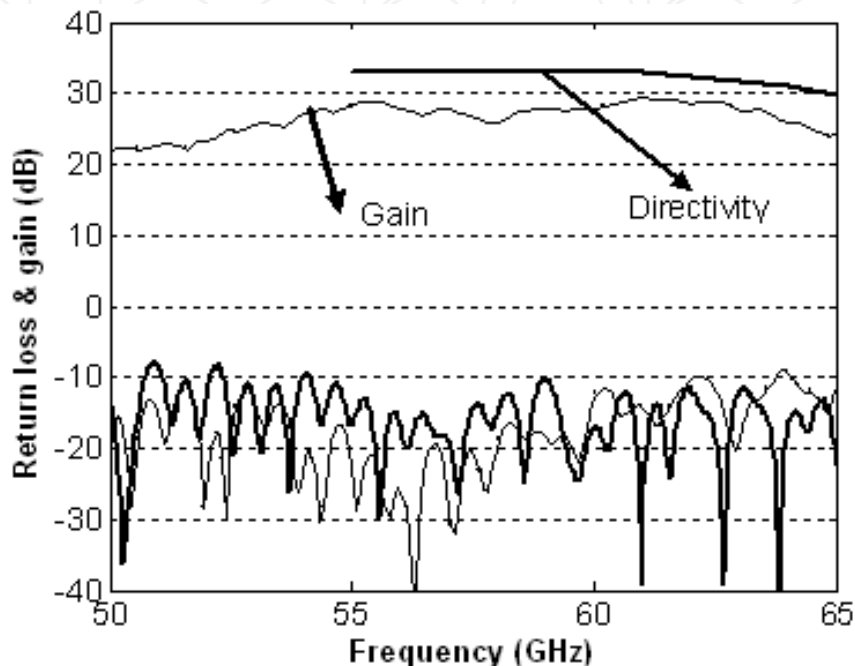


Fig. 30. Variation of S11 and gain for a 16 x 16 superstrate aperture antenna array. Simulation — ; measurement - - - .

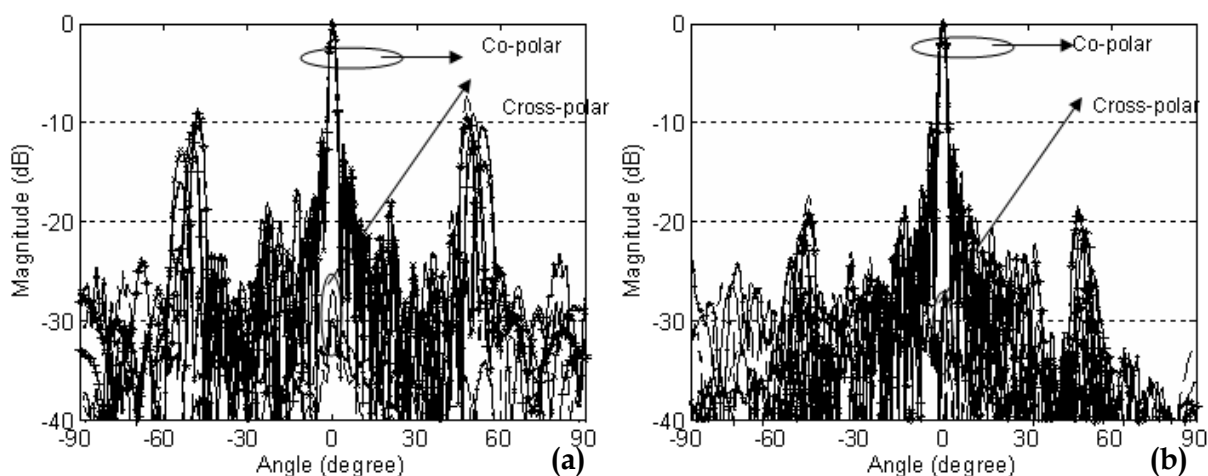


Fig. 31. Measured and simulated E-plane (a) & H-plane (b) radiation patterns of the 2 x 2 superstrate antenna array (Co and Cross polarisation).

57 GHz - Simulated —×— ; 57 GHz - Measured —●— ;  
 60 GHz - Simulated —+— ; 60 GHz - Measured — — — ;  
 62 GHz - Simulated —\*— ; 62 GHz - Measured - - - - .

It is noted from the study that single/small array superstrate antenna technology is very good for high gain, wide bandwidth and high efficiency, but is not suggestive for big arrays because of the gain go up is not upto the point but is good in terms of efficiency.

### 3. Comparison of superstrate slot coupled antenna with superstrate aperture antenna

Table VI gives the comparison of the superstrate aperture antenna element or antenna array presented with slot coupled superstrate antenna element or antenna array. It is clear that superstrate aperture antenna element / antenna array give broad S11 bandwidth of 15% / 13.3% with better efficiency as compared to superstrate slot coupled antenna element / antenna array. Also the antenna size is smaller compared to the other in both the cases. I.e. superstrate aperture antenna element or antenna array gives sufficient bandwidth, gain and efficiency for 60 GHz applications.

Antenna	Return loss bandwidth (measured)	Maximum gain (measured)	Efficiency Estimated $\eta$	Size
Single superstrate Aperture	15%	13.1	79%	6 mm x 13.5 mm x 3.48 mm
Single superstrate slot coupled	6.8%	14.6	76%	10 mm x 10mm x 3.48 mm
2x2 superstrate Aperture	13.3%	16.6	74%	13 mm x 20 mm, x 3.48 mm
2x2 superstrate slot coupled	6.7%	16	63%	16 mm x 16 mm x 3.48 mm

Table VI. Comparison between superstrate aperture s antenna and slot coupled superstrate antenna explained in section 2.

### 4. Conclusion

In this chapter we explained about the significance of superstrate on antenna performance at millimeter wave frequencies. It is found that the size of the superstrate is critical, which is not the case in lower frequencies. Also we studied the antenna performance with different source of excitation. It is noted that superstrate technology is very good for a single patch and also for small array but not that much good for big arrays. As a conclusion, it is found that superstrate aperture antenna element / antenna array is a good candidate for wideband, high gain and high efficiency antenna design in millimetre wave range. Moreover it is easy to integrate with electronics by placing the feed on backside of the substrate where the electronic components are integrated, and the radiating aperture and superstrate (i.e. the radiation part) are on the other side.

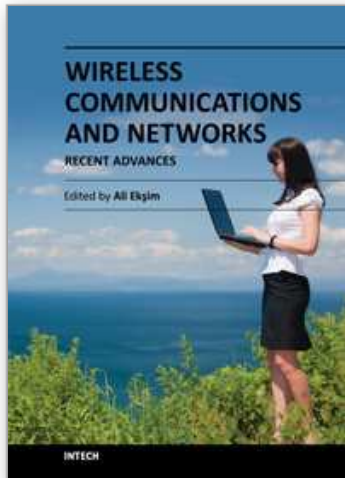
## 5. References

- Cho, W; Yong Hei Cho; Cheol-Sik Pyo & Jae-Ick Choi. (2003). A high gain microstrip patch array antenna using a superstrate layer, *ETRI journal*, 2003, vol. 25, pp.407-411.
- Gupta, R. K. & Kumar, G. (2005). High gain multilayered antenna for wireless applications, *Microw. Opt. Technol. Lett.*, vol. 50, no. 7, pp. 152-154, Jul. 2005.
- Julio-Navarro. (2002). Wide-band, low-profile millimeter wave antenna array, *Microw. Opt. Technol. Lett.*, 2002, vol. 34 , pp. 253-255.
- Kärnfelt, C; Hallbjörner, P; Zirath, H. & Alping, A. (2006). High gain active microstrip antenna for 60-GHz WLAN/WPAN applications, *IEEE Trans. on Microw. Theor. and Techniq.*, Jun. 2006, 54 (6), pp. 2593-2602.
- Liu, D; Gaucher, B; Ullrich, P. & Janusz, G. (2009). *Advanced Millimeter-wave technologies*, (Wiley, 2009), pp. 170-172.
- Lafond, O. (2000). Conception et Technologies D'antennes imprimees Multicouches a 60 GHz, *PhD thesis, University of Rennes1, France*, Dec. 2000, pp. 52-54
- Lafond, O; Himdi, M. & Daniel J. P. (2001). Thick slot-coupled printed antenna arrays for a 60 GHz indoor communication system, *Microw. Opt. Technol. Lett.*, 2001, vol. 28, pp. 105-108.
- Meriah, S. M; Cambiaggio, E; Staraj, R. & Bendimerad, F. T. (2008). Gain enhancement for microstrip reflect array using superstrate layer, *Microw. Opt. Technol. Lett.* , 2008, vol. 46, pp. 1923-1929.
- Menudier, C; Thevenot, M, Monediere, T & Jecko, B . (2007). Ebg resonator antennas state of the art and prospects, *International Conference on Antenna Theory and Techniques*, 17-21 September, 2007, Sevastopol, Ukraine.
- Nesic, A; Nesic, D; Brankovic, V; Sasaki, K. & Kawasaki, K. (2001). Antenna solution for future communication Devices in mm-wave range, *Microwave Review*, pp. 9-17, Dec. 2001.
- Soon-soo oh; John Heo; Dong-Hyeon Kim; Jae-Wook Lee; Myung-sun song & Yung-sik kim. (2004). Broadband millimeter-wave planar antenna array with a waveguide and microstrip feed network, *Microw. Opt. Technol. Lett.*, 2004, vol. 42, pp. 283-287.
- Vettikalladi, H; Lafond, O. & Himdi, M. (2009a). High-Efficient and High-Gain Superstrate Antenna for 60 GHz Indoor Communication, *IEEE Antennas and Wireless Propagation Letters* vol. 8, pp. 1422-1425, 2009.
- Vettikalladi, H; Lafond, O. & Himdi, M. (2009b). High-Gain Broad-band Superstrate Millimeter wave Antenna for 60 GHz Indoor Communications, *5th ESA Workshop on Millimetre Wave Technology and Applications and 31st ESA Antenna Workshop*, 18 - 20 May 2009, ESTEC, Noordwijk, The Netherlands.
- Vettikalladi, H; Le Coq, L; Lafond, O. & Himdi, M. (2010a). Efficient and High-Gain Aperture Coupled Superstrate Antenna Arrays for 60 GHz Indoor Communication Systems, *Microwave and Optical Technology Letters*, 2010.
- Vettikalladi, H; Le Coq, L; Lafond, O. & Himdi, M. (2010b). Wideband and High Efficient Aperture Antenna with Superstrate for 60 GHz Indoor Communication Systems, *2010 IEEE AP-S International Symposium on Antennas and Propagation and 2010 USNC/CNC/URSI Meeting in Toronto, ON, Canada*, on July 11- 17, 2010.

- Vettikalladi, H; Le Coq, L; Lafond, O. & Himdi, M. (2010c). Broadband Superstrate Aperture Antenna for 60 GHz Applications, *European Microwave Week*, 26th sept. to-1st October 2010, Paris, France.
- Zhang, Y.P & Wang, J.J. (2006). Theory and analysis of differentially-driven microstrip antennas, *IEEE Trans. Antennas Propag.*, 2006, vol. 54, pp.1092-1099.

IntechOpen

IntechOpen



## **Wireless Communications and Networks - Recent Advances**

Edited by Dr. Ali Eksim

ISBN 978-953-51-0189-5

Hard cover, 596 pages

**Publisher** InTech

**Published online** 14, March, 2012

**Published in print edition** March, 2012

This book will provide a comprehensive technical guide covering fundamentals, recent advances and open issues in wireless communications and networks to the readers. The objective of the book is to serve as a valuable reference for students, educators, scientists, faculty members, researchers, engineers and research strategists in these rapidly evolving fields and to encourage them to actively explore these broad, exciting and rapidly evolving research areas.

### **How to reference**

In order to correctly reference this scholarly work, feel free to copy and paste the following:

Hamsakutty Vettikalladi, Olivier Lafond and Mohamed Himdi (2012). Superstrate Antennas for Wide Bandwidth and High Efficiency for 60 GHz Indoor Communications, *Wireless Communications and Networks - Recent Advances*, Dr. Ali Eksim (Ed.), ISBN: 978-953-51-0189-5, InTech, Available from:

<http://www.intechopen.com/books/wireless-communications-and-networks-recent-advances/superstrate-antennas-for-wide-bandwidth-and-high-efficiency-for-60-ghz-indoor-communications>

# **INTECH**

open science | open minds

### **InTech Europe**

University Campus STeP Ri  
Slavka Krautzeka 83/A  
51000 Rijeka, Croatia  
Phone: +385 (51) 770 447  
Fax: +385 (51) 686 166  
[www.intechopen.com](http://www.intechopen.com)

### **InTech China**

Unit 405, Office Block, Hotel Equatorial Shanghai  
No.65, Yan An Road (West), Shanghai, 200040, China  
中国上海市延安西路65号上海国际贵都大饭店办公楼405单元  
Phone: +86-21-62489820  
Fax: +86-21-62489821



© 2012 The Author(s). Licensee IntechOpen. This is an open access article distributed under the terms of the [Creative Commons Attribution 3.0 License](#), which permits unrestricted use, distribution, and reproduction in any medium, provided the original work is properly cited.

IntechOpen

IntechOpen